3-11-2020 1:00 PM

Generation of Conditional Ku70 Knockouts in Human Cell Lines Using CRISPR/Cas9 and Dual-Nuclease CRISPR/TevCas9

Gursimran Parmar, *The University of Western Ontario*

Supervisor: Schild-Poulter, Caroline, *The University of Western Ontario*
Co-Supervisor: Edgell, David, *The University of Western Ontario*
A thesis submitted in partial fulfillment of the requirements for the Master of Science degree in Biochemistry
© Gursimran Parmar 2020

Abstract

The Ku heterodimer, Ku70 and Ku80, plays a key role in DNA repair. Viable Ku70 knockouts exist in mice but not in human cell lines. The objective was to create Ku70 knockouts and evaluate knockout viability in human cells using CRISPR/Cas9 and TevCas9. Editing is achieved by Cas9 through one sequence-specific blunt cut accompanied by error-prone DNA repair. However, TevCas9, a novel fusion protein of Cas9 and I-Tev, creates two non-compatible DNA breaks and biases editing events towards a small deletion. Ku70 has five processed pseudogenes therefore intron-exon junctions were targeted by gRNA and a cell line stably transfected with an inducible second copy of Ku70-HA was used to compensate for the loss of endogenous Ku70. After transfection with Cas9 or TevCas9, monoclonal cell lines were picked. Analysis showed lowered or absent Ku70 expression. These Ku knockouts can be used to determine if Ku is required for human cell viability.

Keywords

Summary for Lay Audience

The Ku protein, composed of two smaller proteins, Ku70 and Ku80, is important for maintaining the integrity of DNA, through its function in DNA repair. There may be additional functions for Ku in human cells as previous studies have reported that deleting Ku from human cells caused cell death suggesting that Ku is essential in human cells. The goal of this project is to generate a knockout cell that does not contain Ku70 to further study the role of Ku and to evaluate whether removing Ku70 will kill human cells or not. CRISPR/Cas9 is a popular tool used to remove a protein of interest from cells and gather knowledge on the protein by seeing the effect of removing it on the cell. TevCas9 is a variation of Cas9 that may be more effective and precise. We wanted to compare the efficiencies of Cas9 and TevCas9. Initially, trying to knockout Ku70 in immortalized human cells was unsuccessful. To test whether this meant Ku70 was essential or CRISPR-Cas9 was non-functional, we created a cell line with a second copy of the Ku70 that can be turned on and off when needed. If removing Ku70 is lethal, the second copy will produce some Ku70 protein that will keep the cell alive. This will allow the first copy to be safely removed by CRISPR without killing the cells. Subsequently, we will turn off the second copy too and observe whether cells can survive in the complete absence of Ku70. The generation of these cells will serve as the basis for studies investigating other roles of Ku outside well-known DNA repair and whether Ku has essential functions in human cells.

Co-Authorship Statement

This thesis was written entirely by Gursimran Parmar and was edited by Dr. Caroline Schild-Poulter and Dr. David Edgell. All experiments contributing to this thesis were performed by Gursimran Parmar except for the following:

- Cas9 and TevCas9 plasmid constructs were created by Jasmine Therrien and Dr. Thomas McMurrough
- pBIG Ku70 plasmid construct was created by Elizabeth Walden
- Screening of HEK293 TREX Ku70-HA potential knockouts was conducted by Rachel Kelly

Acknowledgments

I would first like to thank my project supervisors, Dr. David Edgell and Dr. Caroline Schild-Poulter for all your expert guidance throughout my masters. I am very grateful to my committee members, Dr. Dean Betts and Dr. Murray Junop, for your insightful critiques, suggestions, and encouragements. I would also like to thank Dr. Junop's lab for providing me with the HEK293 TREX cell line.

I would like to thank all the members of the Edgell Lab and Schild-Poulter lab for your assistance when I had questions and for your advice in overcoming the many obstacles in my research. I would like to especially thank Sanna Abbasi and Jasmine Therrien for your one-on-one mentorship and feedback and Xu Wang for your lab expertise that helped me greatly throughout this project. Last, but not least, I would like to express my gratitude to my family for your unwavering support. I am truly thankful for everyone who has been a part of this memorable journey.

Table of Contents

List of Tables

List of Figures

List of Abbreviations

BioID – Proximity-dependent biotin identification

bp – base pair

CRISPR – Clustered regularly interspaced short palindromic repeats

crRNA – CRISPR RNA

DAPI – 4′,6-diamidino-2-phenylindole

DMEM – Dulbecco's Modified Eagle's medium

DNA – Deoxyribonucleic acid

DNA-PK – DNA-dependent protein kinase complex

DNA-PKcs – DNA-dependent protein kinase catalytic subunit

DSB – Double-stranded break

dsDNA – Double-stranded DNA

FACS – Fluorescence activated cell sorting

FBS – Fetal bovine serum

GFP – Green fluorescent protein

gRNA – Guide RNA

HA – Human influenza hemagglutinin

HBS – HEPES-buffered saline

HDR – Homology-directed repair

HEPES – Hydroxymethyl piperazineethanesulfonic acid

hetKO – Heterozygous knockout

HR – Homologous recombination

Indel – Insertion or deletion

IR – Ionizing Radiation

mRNA – Messenger RNA

NHEJ – Non-homologous end joining

PAM – Protospacer adjacent motif

PBS – Phosphate-buffered saline

PCR – Polymerase chain reaction

PDB – Protein Data Bank

PP – Processed pseudogenes

RNA – Ribonucleic acid

RNP – Ribonucleoprotein

ROS – Reactive oxygen species

RPE1 – human retinal pigmented epithelial

SaCas9 – Staphylococcus aureus Cas9

SDS-PAGE – Sodium dodecyl sulfate-polyacrylamide gel electrophoresis

SpCas9 – Streptococcus pyogenes Cas9

T7E1 – T7 Endonuclease I

TBS-T – Tris-buffered saline with Tween-20

Tet-OFF – Tetracycline-off

Tet-ON – Tetracycline-on

TIDE – Tracking of indels by decomposition

tracrRNA – Trans-activating crRNA

WT – Wild type

XRCC5 – X-ray cross complementing protein 5

XRCC6 – X-ray cross complementing protein 6

Chapter 1

1 Introduction

1.1 DNA Damage

Cells are continuously at risk of deoxyribonucleic acid (DNA) damage by exogenous and endogenous agents. For instance, on average, cell genomes are targets of tens of thousands of lesions daily (1). Lesions can be caused by exogenous environmental agents such as ultraviolet light, ionizing radiation (IR) and chemicals, including tobacco smoke and aflatoxins (2). People are exposed to natural radiation sources on a daily basis (3) and these naturally occurring environmental factors, such as IR, are difficult to avoid. Even in the absence of exogenous factors, DNA damage can also occur through endogenous agents such as dysfunctional topoisomerase I and II activity during DNA replication, reactive oxygen species (ROS), a by-product of the electron transport chain, and reactive nitrogen compounds, produced in immune cells as a response to inflammation (2, 4, 5). Although DNA damage is common, if left unrepaired or repaired incorrectly, it can lead to mutations in the genome that may be passed on to progeny or disrupt vital cellular function such as DNA replication (2). Thus, the cell has acquired several DNA repair responses to combat various forms of DNA lesions. Genetic defects in these DNA repair responses are linked to mutagenesis, immunodeficiency, and malignancy, highlighting their importance in genome stability (6).

While cell responses to DNA damage are specific to the type of lesion, all these pathways follow a similar general scheme which relies on DNA damage sensors to correctly detect lesions, followed by signalling cascades and activity of repair factors (2). Some specific forms of lesions can be repaired by direct enzyme-mediated reversal, namely, photolyase-, alkyltransferase-, and dioxygenase-mediated repair processes (7); however, most are repaired by pathways with multiple sequential steps. Common forms of DNA damage are base lesions, protein-DNA crosslinks, interstrand crosslinks and single-stranded DNA breaks. These lesions are effectively repaired by a multitude of pathways: base-excision repair, mismatch repair, single-stranded break repair and nucleotide

excision repair (8–10). The majority of these repair processes include nucleases to resect damaged DNA ends, polymerases to close the gaps, and ligases to rejoin the DNA backbone (3). In some cases, lesions persist despite these repair mechanisms and can block DNA replication. To avoid deadly stalling of the replication fork, error-prone and low fidelity translesion DNA polymerases are used to bypass the lesion site (11).

1.2   Double-Stranded Break Repair

A less common but highly cytotoxic type of DNA damage is a double-stranded break (DSB), where there is a simultaneous break in the sugar-phosphate backbones of two complementary DNA strands. They must be repaired immediately to preserve chromosomal integrity. If left unrepaired, DSBs can lead to DNA loss and deadly chromosomal translocations. While most forms of DSBs are pathological, there are physiological cell processes that rely on controlled creation and repair of DSBs. DSBs play an important function in V(D)J recombination, the process responsible for creating diversity in variable regions of immunoglobulins and T cell receptors (12). Topoisomerase II relies on DSBs to control the supercoiled state of DNA (13) and DSBs are required during recombination during gamete formation, specifically for the resolution of the Holliday junction that forms during crossover events in prophase I during meiosis (14). Pathological forms of DSBs are caused most frequently during DNA replication when DNA is unwound and vulnerable. The majority of spontaneous DSBs occur by replication across a nicked chromatid during S phase, creating a chromatid break (15). The second most prevalent cause of DSBs is ROS followed by IR, and then by mechanical stress on chromosomes (3).

The cell has two principal mechanisms of DNA repair to address DSBs. In replicating organisms in the S phase, including replicating bacteria and replicating haploid yeast, homology-directed repair (HDR) is the favoured option (3), namely homologous recombination (HR) and single-strand annealing. All forms of HDR use the complementarity of the sister chromatid to faithfully repair the DSB (16, 17).

In cases of DSBs in non-replicating haploid organisms and diploid organisms outside of the S and G2 phase, homologous DNA is not available nearby to function as a template.

For these situations, cells acquired another form of DSB repair early in evolution, called non-homologous end joining (NHEJ) (11). The remarkable aspect of NHEJ is its ability to recognize and join ends together with a wide range of overhang length, DNA end sequence, and DNA end chemistry (3). Similar to most DNA repair pathways, NHEJ pathways consist of a DSB sensor, nucleases, polymerases and ligases (18).

1.3   The Ku Heterodimer

At the beginning of NHEJ, the first protein to be recruited to the DSB is the Ku heterodimer (Figure 1.1). It is a DNA binding protein, comprised of two subunits, Ku70 (X-ray cross complementing protein 6 [XRCC6]) and Ku80 (X-ray cross complementing protein 5 [XRCC5]) (17). Ku70 and Ku80 appear to be obligate heterodimers. This is supported by previous mouse knockout studies that found the knockout of either subunit in Ku results in a drop in abundance of the other to negligible levels, suggesting subunit dimerization may have a stabilizing effect (19, 20). Overall, the knockout of either Ku70 or Ku80 leads to functional knockout of the Ku heterodimer.
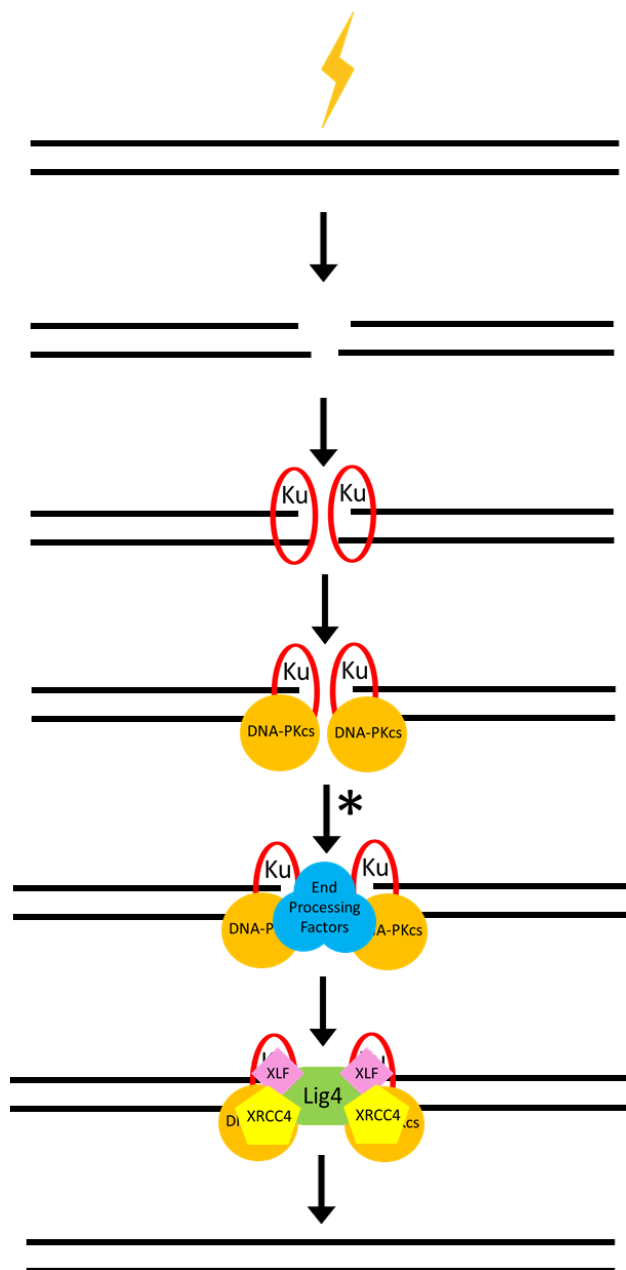
Figure 1.1: Schematic representation of non-homologous end joining. The Ku heterodimer is the first protein to arrive at a DSB and recruits DNA-PKcs. Together with DNA, these factors form the DNA-PK complex. This initial repair complex then recruits factors required for end-processing and ligation. *The exact order of recruitment of end-processing and ligating factors is not known at this time. It is possible that processing enzymes and ligases get recruited at an earlier stage in the NHEJ process (21).

The Ku heterodimer is evolutionarily conserved in prokaryotic and eukaryotic organisms. Ku70 and Ku80 do not have similar primary sequences however they share a conserved secondary and tertiary structure (17, 22). Both subunits bind to each other and form an asymmetrical basket structure with the basket handle being formed by a ring capable of binding DNA ends (Figure 1.2A, B). The ring is lined with positively charged basic residues that favourably interact with the negatively charged sugar-phosphate DNA backbone. This allows Ku to bind dsDNA ends with high affinity ($K_d = 10^{-9}$ M), and circular and single-stranded DNA ends with much lower affinity (17).

In mammals, Ku is a highly conserved and abundant protein. In humans, an estimated 500,000 Ku molecules are present in a single cell at any given time (17). Mammalian cells spend the majority of their life cycle in the G1 phase, therefore NHEJ functions as the main dsDNA repair pathway (23).

Unlike HR that is primarily active during S and G2 phases, NHEJ can be utilized at any point in the cell cycle and has the capacity to join almost any two DNA ends together. The first step in the NHEJ repair pathway is the recognition of a DSB by Ku (Figure 1.1). Ku binds the dsDNA ends in a sequence-independent manner then proceeds to act as a scaffold, interacting with several NHEJ factors and processing enzymes to facilitate the construction of a DNA repair complex (17). Ku translocates along the DNA and recruits DNA-dependent protein kinase catalytic subunit (DNA-PKcs) to generate the DNA-dependent protein kinase complex (DNA-PK), followed by several auto- and trans-phosphorylation events of the DNA, Ku and DNA-PKcs itself (Figure 1.1). The formation of this complex shields against exonucleolytic processing of DNA ends and minimizes DNA loss (24). Next, Ku mediates recruitment of factors necessary for end-processing (Figure 1.1) (25). DSB can result in DNA strands having blunt ends, 5' or 3' overhangs, 3' phosphoglycolate termini and DNA adducts. Damaged ends may require kinases/phosphatases to restore 5′-phosphates required for ligation and/or remove unligatable 3′-phosphates (26). Depending on the cause and type of DSB, Ku, directly and indirectly, is responsible for recruiting the correct combination of kinases, nucleases and polymerases required to produce two compatible DNA ends for ligation. Finally, Ku is required for the recruitment of the ligase complex,

A **B**
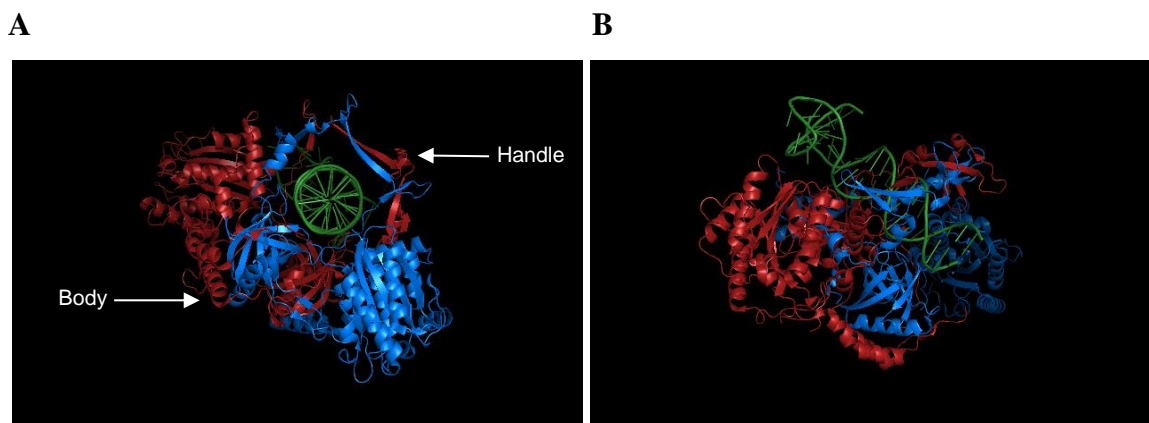
Figure 1.2: Crystal structure of the Ku heterodimer. Ku70 [blue]/Ku80 [red]) bound to DNA (green). Structure from Protein Data Bank (PDB; PDB ID = 1JEY) **(A)** Basket structure (white labels and arrows) is visible at this top-down view of the DNA helix, with DNA (green) bound through the ring. **(B)** Side view of DNA (green) bound through the ring structure.

composed of ligase IV, XRCC4 and XLF (Figure 1.1) (18). The exact timing and order of recruitment of end-processing and ligating factors is not well characterized. Processing enzymes and ligases may get recruited at an earlier stage of NHEJ by DNA-PK and not necessarily in that order (20). After ligation, it is not quite clear how Ku molecules are removed now that DNA ends, bound through its ring structure, are ligated together. Data from *Xenopus laevis* and human cell cultures indicate that ubiquitin-mediated degradation of Ku80 is important for successful repair of DSBs (27, 28). In yeast, there is evidence for DNA nicking mechanisms that allow Ku to be freed that is mediated by an HR complex, Mre11-Rad50-Xrs2 (29).

Experiments conducted in yeast also show that the deletion of Ku results in telomere shortening, suggesting that Ku also interacts with telomeres and plays an important role in determining telomere length. The mechanism through which Ku interacts with telomeres appears to be primarily through promoting the association of telomerase with telomeres (30–32). This mechanism is separate from NHEJ as DNA ligase IV deficiency, a protein essential for NHEJ, does not result in altered telomere length in yeast and mammalian cells (33, 34).

1.4   Ku Knockdown and Knockout Studies

Both Ku70 and Ku80 knockout mouse cell lines have been established as well as knockout mice and these have been used to gain insight into Ku function. Ku deficient mice have been shown to live one-third of the lifespan of wild type (WT) mice with increased senescence and cancer incidences (17, 35). Decreased NHEJ, shorter telomeres and increased genome instability may contribute to this phenotype. Interestingly, Ku knockout mice are also dwarfs compared to WT, suggesting Ku may function to regulate cell growth. Evidently, there are many cellular roles of Ku yet to be discovered.

The following work will focus on Ku in human cells. Thus far, there are no human Ku homozygous knockout cell lines available to study the role of Ku in human cells. Many knockdown studies have successfully knocked down Ku70/80 to low levels in many different human cell lines: human mammary epithelial cell line (36), human proneural cell lines (37), and CD4$^+$ T cells (38).

Ku knockouts have previously been attempted in a human colon cancer cell line, HCT116, targeting Ku80 (39). They were able to create heterozygous knockouts (hetKO) that displayed slower cell proliferation, shortened telomere, and hypersensitivity to IR. Homozygous knockouts, created by functional inactivation of the remaining Ku80 copy in hetKOs, were not viable, dying shortly after inactivation. Ku70 knockouts were later attempted in HCT116 and Ku70 hetKOs displayed similar phenotype as Ku80 hetKOs: decreased proliferation, shorter telomeres, and IR hypersensitivity. As such, Ku70 homozygous knockout could not be achieved (40, 41). These results suggest that Ku80, and Ku70, may be essential for survival (39–41).

These knockout studies suggest that Ku may be essential in human cells. This is also supported by another knockout study conducted in near-haploid human cell lines (HAP1 and KBM7) that contain only one copy of most chromosomes, including chromosome 22, which carries the Ku70 gene. Results indicate that Ku70 knockouts were lethal in both cell lines (42). Furthermore, while several human disorders have been linked to mutations in many NHEJ factors, no disease has been characterized where Ku subunits have been mutated (17).

Considering this data, it is quite possible that Ku is essential in humans. However, we believed that further knockout studies would be valuable, particularly in non-cancerous and diploid human cell lines. It is possible that cancerous cell lines may have increased dependence on Ku due to increased genome instability. Thus work here focused on the generation of Ku knockouts by targeting the Ku70 gene in HEK293 cells, an immortalized but non-cancerous cell line derived from human embryonic kidney cells (43). HEK293 cells, although considered non-cancerous, are tetraploid for chromosome 22, where the XRCC6 gene is located (44). Therefore, knockout experiments were also attempted in human retinal pigmented epithelial (RPE1) cells, a telomerase immortalized human cell line with a stable diploid genome. They display growth characteristics, and gene expression patterns comparable to young normal cells (45).

1.5   Origins of the CRISPR/Cas9 System

A prevalent genome editing tool used to create gene knockouts is the clustered regularly interspaced short palindromic repeats (CRISPR)/Cas9 system. The CRISPR/Cas9 system, first discovered in *Streptococcus pyogenes,* evolved as a form of the bacteria's adaptive immunity against plasmids and phages (46). In prokaryotes, this system functions as a complex comprised of a nuclease, Cas9, and a two-ribonucleic acid (RNA) structure composed of mature CRISPR RNA (crRNA), which recognizes viral DNA, and trans-activating crRNA (tracrRNA), which connects crRNA to Cas9. Fragments of foreign plasmid or phage DNA, called protospacers, are integrated into the host genome at CRISPR loci from which the crRNA is transcribed. The crRNA is processed to yield small mature crRNAs that form a complex with tracrRNA and Cas9 and are used target exogenous viral and phage DNA for cleavage from where the crDNA originated from (46). This is analogous to the human adaptive immune system where after exposure to an antigen either from a pathogen or a vaccine, the human body commits the antigen to immunological memory through activated B-cells and T-cells that give rise to a more powerful and efficient immune response upon re-exposure (47). Similarly, with CRISPR, after a phage attack, viral DNA is preserved by the bacteria and used as a template to quickly recognize and target future attacks by the same virus. The bacteria are able to avoid targeting their own genome through the protospacer adjacent motif (PAM). This short sequence (5'-NGG-3') must be present downstream of the target site (site complementary to crRNA) for Cas9 to cleave. By eliminating all PAM sequences from its CRISPR loci, the bacteria are able to distinguish exogenous from endogenous DNA (48).

This system has been adapted from *S. pyogenes* to produce a powerful genome editing tool. By engineering the two RNA structures together (crRNA + tracrRNA) to create one RNA chimera (guide RNA), the system has been simplified to an easily programmable protein:RNA complex (46).

1.6   Gene Editing Tool: CRISPR/Cas9

The CRISPR/Cas9 system has emerged as the most popular tool for genome editing. The fusion of crRNA and tracrRNA to make a single guide RNA (gRNA) was an important breakthrough. It gave scientists the ability to easily program the Cas9 complex to have various targets through the modification of the gRNA sequence (46). During gene editing, Cas9 protein forms a complex with gRNA *in vivo*. CRISPR gRNA is a small RNA fragment that contains sequence that binds to Cas9 and sequence that is complementary to the site targeted in the genome. After gRNA binds to Cas9 and a ribonucleoprotein (RNP) forms, the gRNA guides the RNP to the targeted site. Once bound to DNA, the Cas9 protein scans the DNA 3' of the target site for the PAM sequence, 5' NGG 3' (49). If there is a PAM sequence present, then Cas9 creates a blunt dsDNA break 3 base pairs (bp) upstream of the PAM sequence. Upon the dsDNA break, the blunt ends undergo either error-prone NHEJ or high-fidelity HR, the two main dsDNA repair pathways.

The DSB can be ligated back together, which regenerates the target site until there is exonucleolytic processing of the DNA ends that results in an insertion or a deletion (indel). A small repair template can be provided for specific HDR to occur at the break site for applications such as specific gene editing. However, non-homologous end joining, the major DNA repair pathway in humans, with its ability to perform error-prone repair while creating a variety of indels is sufficient for producing knockout genes. The result is a heterogeneous population with numerous genomic modifications of various sizes of indels. Some of these indels can lead to frameshift mutations that may result in a knockout of the gene (50). The advantage of this system, contributing to its importance and prevalence, is its ease of programmability. The gRNA can be designed to target any site in the gene that is followed by the PAM sequence (5' NGG 3').

Another version of the CRISPR/Cas9 system has been discovered in *Staphylococcus aureus*. Some advantages of *S. aureus* Cas9 (SaCas9) over *S. pyogenes* Cas9 (SpCas9) is its small size, 1053 amino acids compared to 1369 amino acids and a longer PAM sequence, 5'-NNGRRT-3' as opposed to 5'-NGG-3' (51). Its smaller size increases the

utility of SaCas9 in research and although the larger PAM limits the number of possible target sites, it also results in less off-target sites, a major area of concern for SpCas9 (52).

1.7   Gene Editing Tool: CRISPR/TevCas9

An RNA-guided dual nuclease, TevCas9 is another genome editing nuclease that builds on the CRISPR/Cas9 system. Created by the Edgell lab, TevCas9 is a fusion protein comprised of the monomeric nuclease and linker domain of a homing nuclease, I-TevI and the nuclease domain of Cas9 (53). TevCas9 is an improvement on the Cas9 system in many ways. It is comprised of two nuclease domains that both cleave in a sequence-dependent manner which results in deletions of defined lengths in the range of 33 to 36 bp (53).

I-TevI is a site-specific, sequence-tolerant homing endonuclease, encoded by a group I intron in the thymidylate synthase gene of bacteriophage T4. As a monomer, it has the ability to cleave and produce a 3' two base overhang (54, 55). Thus, when linked to the Cas9 nuclease domain, the complex produces two cleavage events, one blunt cleavage by Cas9 domain and one 3' overhang by Tev domain. The Cas9 nuclease domain relies on gRNA to recognize the target site and functions identical to the protein, Cas9, creating one blunt DSB. The I-TevI nuclease domain has a recognition sequence of 5' CNNNG 3' and it cleaves on the N-terminus side of guanine producing a 2 bp long, 3' overhang. Therefore, cleavage with TevCas9 creates two non-compatible ends, minimizing the possibility of a regenerated target site (53). In contrast, Cas9 stimulates only a single blunt DSB (49). The TevCas9 system offers the same ease of programmability of the Cas9 system to select and cleave at a target site. Following discovery of SaCas9, the I-TevI nuclease domain has also been fused with SaCas9 to give TevSaCas9.

One application of TevCas9 is the ability to cleave in an exon while targeting gRNA to an intron close to an intron-exon junction. TevCas9 stimulates a DSB in the intron through its Cas9 nuclease domain. Additionally, the I-TevI nuclease domain also cleaves in the exon preceding that intron. This is the central strategy that will be used by this work to knock out Ku70.

1.8   Processed Pseudogenes

Ku70 is extremely abundant in human cells (17). The problem is that highly expressed genes are often prone to producing processed pseudogenes (PP) (17, 56). PPs are created in germline cells through the reverse transcription and integration of messenger RNA (mRNA) into random locations in the genome (56, 57). Highly expressed genes require the production of large amounts of mRNA. This can result in the generation and integration of one or multiple pseudogenes into the genome. These PPs are often non-functional and have lost the ability to produce proteins (56, 58).

This is the case with the Ku70 gene. Ku70 is located on chromosome 22. However, it has five pseudogenes present in the human genome (XRCC6P1-5). Three pseudogenes are found on chromosomes 1, 8 and 10 and two pseudogenes are both found on chromosome X. Consequently, it is not possible to directly target a Ku70 exon as there may be up to five identical sites present on other chromosomes. Multiple DSBs on the same or different chromosomes can result in mutagenic or lethal chromosomal rearrangements, such as translocations (59). As PPs are generated by reverse transcription of mRNA, these pseudogenes do not contain the intronic region found in the original gene. Therefore, to knockout Ku, it is necessary to target an intron, ensuring that none of its pseudogenes are targeted.

1.9   Objectives

1. To generate viable Ku70 knockouts in HEK293 cells: If Ku70 knockout cells are viable, cell lines will be phenotypically characterized. If we cannot knockout Ku, then the goal is to demonstrate that Ku70 is required for human cell viability.

2. To demonstrate that targeting the intron-exon junction is a feasible strategy to disrupt Ku70: If successful, the knockout strategy employed in this work can be generalized to knockout other highly expressed genes that may have multiple pseudogenes present in the genome. PPs do not contain introns; thus, intron region from the original gene near an intron-exon junction is an ideal target. With TevCas9, it is possible to get cleavage in the exon itself, while only targeting the

intron. With Cas9, this is much less likely and depends solely on exonucleolytic processing to create deletions large enough to extend into the exon, demonstrating TevCas9 is both necessary and sufficient in addressing more challenging knockout targets.

1.10 Rationale: Target Site

The strategy was to target an intron just upstream to an intron-exon junction in Ku70 (Figure 1.3A, B). While working with SpCas9, the junction between exon 10 and the subsequent intron was targeted (Figure 1.3A). When working with SaCas9, three intron-exon junctions were simultaneously targeted (Figure 1.3B). A gene knockout can be achieved through partial exon deletions stimulated by dual cuts made by TevCas9. With Cas9, the knockout efficiency depends on error-prone NHEJ and the possibility of large deletions that may extend from the cleavage site in the intron to the preceding exon (Figure 1.3B).

1.11 Conditional Knockout: Strategy to Address Lethality of Ku70 Knockouts

Genes essential to cell viability, as Ku70 is suspected to be, cannot be directly knocked out. Therefore, we planned to create conditional Ku70 knockout cells. To address the possibility of lethality, a HEK293 stable cell line containing a human influenza hemagglutinin (HA) tagged exogenous copy of Ku70 (Ku70-HA) under the control of a tetracycline-inducible promoter was used for knockout studies. This second copy of Ku70 was expected to compensate for the loss of endogenous Ku70 and maintain knockout viability. The CRISPR system was used on these stable cells lines to knockout the endogenous copy of Ku70. Once knockouts are obtained, exogenous Ku70-HA expression was shut off. Cell death, under this condition, was used to indicate whether knockout of Ku70 was lethal in HEK293 cells.

A

tatcgttgagaagcttcgcttcacatacaggtgagtcaatctcaggctttctggaactgcctcctg
atagcaactcttcgaagcgaagtgtatgtccactcagttagagtccgaaagaccttgacggaggac

Tev

Exon 10 Intron

gRNA PAM

B

tcatgctctttcattttttactccctcaggttaaagctgaagctcaacaaagatatagtgatctctgtgggcatttata
agtacgagaaagtaaaaaatgaggggagtccaatttcgacttcgagttgtttctatatcactagagacacccgtaaatat

Intron PAM gRNA Tev Exon 7

Figure 1.3: Ku70 sites targeted by gRNA for TevCas9 and Cas9 variants. (A) Ku70 target site for TevSpCas9 and SpCas9. Both nucleases use the same gRNA. The red lines indicate the cleavage sites for both enzymes. Cas9 stimulates one blunt DSB three bp upstream of the PAM sequence. TevCas9 generates two DSB, one 3 bp upstream off the PAM sequence and one in the preceding exon. **(B) Ku70 target site for TevSaCas9 and SaCas9.** The gRNA is targeting the template strand, instead of the coding strand. The PAM site (5'-GGGAGT-3') is present in the intron, thus will not be present in Ku70's pseudogenes. Cas9 cleaves just one bp outside the intron-exon junction, while TevCas9 makes an additional cleavage downstream in the exon.

Chapter 2

2 Methods

2.1 Plasmid Constructs

px458SpCas9$_{GFP}$ (SpCas9-2A-GFP) and px459SpCas9$_{PuroR}$ (SpCas9-2A-puro) vectors were previously obtained from Feng Zhang through Addgene (Addgene plasmid # 48138 and plasmid # 62988) for transfection into mammalian cell lines (50). The nuclease, SpCas9, is linked to green fluorescence protein (GFP) and a puromycin resistance marker, respectively. TevSpCas9 dual nuclease was created by Jason Wolfs by cloning I-TevI (amino acids 1–169) in front of the N terminus of SpCas9 to create px458TevSpCas9$_{GFP}$ and px459TevSpCas9$_{PuroR}$.

The SaCas9 construct was created by Jasmine Therrien. SpCas9 was excised out and full length SaCas9 was cloned into px458SpCas9$_{GFP}$. Polymerase chain reaction (PCR) amplification of the pac gene encoding puromycin N-acetyl-transferase from px459SpCas9$_{PuroR}$ was used to clone puromycin resistance into this construct to create px458$_{PuroR}$SaCas9$_{GFP}$. px458$_{PuroR}$TevSaCas9$_{GFP}$ was constructed by cloning I-TevI (amino acids 1–169) in front of the N terminus of SaCas9 by Dr. Thomas McMurrough.

The pBIG2R-Ku70 tetracycline repressible plasmid was created previously by Elizabeth Walden by cloning full length Ku70 into the multiple cloning site of the pBIG2r vector (60). To allow pBIG2R Ku70 expression to be distinguished from endogenous Ku70 expression, I subcloned an HA-tag to the C-terminus of Ku70 in pBIG2R-Ku70. The pBIG2R-Ku70-HA vector allows for transfection and tetracycline repression of Ku70-HA expression in mammalian cell lines.

To create pcDNA5/FRT/TO-Ku70-HA, for the TREX Ku70-HA tetracycline repressible system, I PCR-amplified full length Ku70-HA from pBIG2R-Ku70-HA using primers containing restriction enzyme sites and cloned it into pcDNA5/FRT/TO.

2.2   Designing gRNA

Since Ku70 has five pseudogenes that contain only exons from endogenous Ku70, gRNA was designed to target intron-exon junctions in Ku70. A script made by Dr. Edgell was used to locate potential Cas9 and TevCas9 target sites in Ku70 (Figure 2.1). This script searched the Ku70 DNA sequence for regions that spanned intron-exon junctions and had to the consensus sequence required for Tev nuclease and Cas9 nuclease cleavage. The consensus sequence for SpCas9 and TevSpCas9 target sites was 5' CNNNG(N)$_{34-40}$NGG 3' and for SaCas9 and TevSaCas9 target sites was 5' CNNNG(N)$_{34-40}$NNGRRT 3'.

5' CNNNG 3' is the consensus sequence required for Tev nuclease cleavage. 5' NNG 3' is the PAM sequence for SpCas9 while 5' NNGRRT 3' is the PAM sequence for SaCas9 required for Cas9 cleavage.

Ku70 knockout was attempted using following gRNAs:

- SpCas9 & TevSpCas9

    o   Target 0: 5' AGTCAATCTCAGGCTTTC 3'

- SaCas9 & TevSaCas9

    o   Target 1: 5' AGCTTCAGCTTTAACCTGA 3'

    o   Target 2: 5' ACTCAGCAGGTGTGCACTCAGC 3'

    o   Target 3: 5' TCATTGCTTCAACCTTGGGCAC 3'

These gRNAs were used to guide the Cas9 nuclease in Cas9 and TevCas9. All of the target sites chosen spanned both intronic and exonic region of the Ku70 gene (Figure 2.1). TevCas9 had an additional cut site present upstream of the gRNA in these target sites determined by the Tev nuclease consensus sequence of 5' CNNNG 3'. Target site 0 was used with SpCas9, thus used the PAM 5' NGG 3'. Target site 1-3 were used with SaCas9, thus use the PAM 5' NNGRRT 3'.

atcgttgagaagcttcgcttcacatacaggtgagtcaatctcaggctttctggaactgcctcctga
tagcaactcttcgaagcgaagtgtatgtccactcagttagagtccgaaagaccttgacggaggac

```
        Tev                         gRNA              PAM
                       TARGET SITE 0
        Exon 10                              Intron
```

tcatgctctttcatttttactccctcaggttaaagctgaagctcaacaaagatatagtgatctctgtgggcatttataa
agtacgagaaagtaaaaaatgagggagtccaatttcgacttcgagttgtttctatatcactagagacacccgtaaatatt

```
                    TARGET SITE 1
        PAM      gRNA                          Tev
Intron                           Exon 7
```

acctgttgcggaaggttcgcgccaaggagaccaggaagcgagcactcagcaggtgtgcactcagcccgggtcagctgcctacactgc
tggacaacgccttccaagcgcggttcctctggtccttcgctcgtgagtcgtccacacgtgagtcgggcccagtcgacggatgtgacg

```
                    TARGET SITE 2
        Tev                    gRNA        PAM
        Exon 6                        Intron
```

ccactcttctgtgttttgattttctagtgcccaaggttgaagcaatgaataaaagactgggctccttggtggatgagtttaagga
ggtgagaagacacaaaactaaaagatcacgggttccaacttcgttacttattttctgacccgaggaaccacctactcaaattcct

```
                    TARGET SITE 3
        PAM      gRNA                Tev
Intron                      Exon 12
```

Figure 2.1: Four target sites used in Ku70 knockout experiments. Target sites were located using a script by Dr. Edgell. They span both the intronic and exonic region of the Ku70 gene. Target site 0 was used with SpCas9, thus used the PAM site 5' NGG 3'. Target site 1-3 were used with SaCas9, thus use the PAM site 5' NNGRRT 3'.

2.3 Golden Gate Assembly

gRNAs were ordered in the form of synthesized oligonucleotides with *Bbs*I cut site compatible overhangs added to each side. The designed gRNA was cloned into px458SpCas9$_{GFP}$, px458TevSpCas9$_{GFP}$, px459SpCas9$_{PuroR}$, and px459SpCas9$_{PuroR.}$ This was accomplished using Golden Gate assembly, following the protocol outlined in Engler *et al.*, 2008 (61). However, the restriction enzyme *Bbs*I was used instead of *Bsa*I. After Golden Gate assembly, heat shock transformation was performed using *Escherichia coli* (DH5α) competent cells to amplify the plasmid. An overnight liquid culture was prepared from individual colonies from the transformation and the next day, the plasmid was purified using EZ-10 Spin Column Plasmid DNA Miniprep Kit by (Bio Basic Inc). Correct gRNA insertion was confirmed by DNA sequencing.

2.4 Tissue Culture of Cell Lines

HEK293 cells (ATCC® CRL-1573) were grown at 37°C in a 5% CO_2 incubator and cultured in Dulbecco's Modified Eagle's medium (DMEM) (Wisent Inc.) to which 8% fetal bovine serum (FBS) (Wisent Inc.), 1% L-glutamine (Wisent Inc.), and 1% sodium pyruvate (Wisent Inc.) were added.

HEK293 TREX cells (Invitrogen Canada Inc.) were gifted by Dr. Murray Junop's Lab. Cells were grown at 37°C in a 5% CO_2 incubator and cultured in DMEM (Wisent Inc.) to which 10% FBS (Wisent Inc.) and 1% L-glutamine (Wisent Inc.), and 1% sodium pyruvate (Wisent Inc.) were added. RPE1 cells (ATCC® CRL-4000) were grown at 37°C in a 5% CO_2 incubator and cultured in DMEM/F-12 medium (Wisent Inc.) to which 8% FBS (Wisent Inc.) and hygromycin B (Wisent Inc.) to the final concentration of 0.01 mg/ml were added.

2.5   Antibiotic Concentrations

Table 2.1. Antibiotic concentrations used for each cell line. Antibiotic concentrations used for selection, maintenance or inducing gene expression categorized by cell line.

ANTIBIOTIC	CELL LINES		
	HEK293	**HEK293 TREX**	**RPE1**
Blasticidin	-	15 μg/mL	5 μg/mL
Doxycycline	0.5 μg/mL**	1 μg/mL **	-
G418	450 μg/mL	450 μg/mL	800 μg/mL
Hygromycin	50 μg/mL	150 μg/mL	10 μg/mL *
Puromycin	1.2 μg/mL	-	2.5 μg/mL
Tetracycline	6 μg/mL **	-	-
Zeocin	-	100 μg/mL	-

(*) indicates concentration for cell maintenance

(**) indicates concentration for gene expression induction

2.6   Transfections

2.6.1   jetPRIME

All jetPRIME transfections were performed using jetPRIME Versatile DNA/siRNA transfection reagent, following the manufacturer's instructions (Polyplus Transfection Inc). Antibiotic was added 24-48 hours after transfection for selection (Table 1).

2.6.2   Lipofectamine

All Lipofectamine transfections were performed using Lipofectamine 3000 transfection reagent, following the manufacturer's instructions specific for 6-well plates (ThermoFisher Scientific Inc). Cells were seeded in 6-well plates 24 hours before transfection to reach 70-90% confluency at time of transfection. Antibiotic was added 48 hours after transfection for selection (Table 1).

2.6.3   Calcium Phosphate

Cells were seeded in a 10 cm dish, 24 hours before transfection to reach 80-90% confluency at time of transfection. One hour before transfection, cell media was replenished with fresh media. During the transfection, 11 ug of DNA was diluted in the appropriate amount of H_2O to reach a final volume of 438 uL. 62 uL of 2M $CaCl_2$ was added to the DNA-H_2O solution. Next, HEPES-buffered saline (HBS) (25 mM hydroxymethyl piperazineethanesulfonic acid (HEPES) pH 7.4, 140 mM NaCl, 6 mM dextrose, 0.75 mM Na_2HPO_4, and 5 mM KCl) was added to the DNA-$CaCl_2$ solution. The final mixture was aerated using a pipet for 1 min, then added dropwise to the cells. Cells were incubated for 18 hours before media was replaced with fresh media. Antibiotic was added 24-48 hours after this step for selection (Table 1).

2.7   DNA Extraction

DNA was extracted from cells using QuickExtract DNA Extraction Solution (Lucigen Corporation). Human cells were harvested and pelleted in an Eppendorf tube at 8000 rpm for 3 minutes. The pellet was washed with phosphate-buffered saline (PBS; Wisent) to remove residual DMEM. The pellet was dissolved in 20-80 uL of QuickExtract solution

using vortexing. The mixture was heated at 65°C for 6 minutes, vortexed for 10 seconds, and heated at 98°C for 2 minutes. The mixture was cooled to room temperature for downstream application.

2.8 Nested Polymerase Chain Reactions

Nested PCR were performed to amplify the TevCas9/Cas9 target site from the extracted genomic DNA (Table 2). Nested PCR were conducted using 2 nested pairs of primers, and 2 consecutive PCR reactions. Nested PCR #1 was conducted using genomic DNA as template and Nest #1 primers for each site. This PCR mixture was then used as the template for Nested PCR #2 that was conducted using Nest #2 primers for each site.

2.9 Cleavage Resistance Assay

Nested PCRs were performed to amplify the TevCas9/Cas9 target site 0 from the extracted genomic DNA (Table 2.2). The final PCR product was 970 bp long. The TevCas9 target site is located at an intron-exon junction. In the target site, there was a cleavage site for the restriction enzyme, *Msl*I. It was located at the edge of the intron-exon junction (Figure 2.2). In this assay, the PCR product was digested with *Msl*I. Digestion produced 2 fragments of 685 bp and 285 bp. If there were any DNA modifications in the *Msl*I cut site, it resulted in resistance to cleavage by *Msl*I. Cleavage products were visualized using gel electrophoresis.

Table 2.2. Primers for nested PCR.

	Sequence	T_m (°C)	PCR product
Target Site 0			
Nest #1 forward primer	ctgtaatcccagcactttgg	56.1	1182 bp
Nest #1 reverse primer	gcaggctctgagagttggtc	58.6	
Nest #2 forward primer	ccccatctttaccgaaagtac	56.2	970 bp
Nest #2 reverse primer	caatcaaggagaagggcg	57.7	
Target Site 1			
Nest #1 forward primer	gagcaccgacctaatgttc	53.0	812 bp
Nest #1 reverse primer	ccccagtcgatccagtctc	57.0	
Nest #2 forward primer	gggttgggaatattcaaccag	53.5	694 bp
Nest #2 reverse primer	gtcacatgcctgtgatccc	55.9	
Target Site 2			
Nest #1 forward primer	cagatggccatgccatta	52.6	1657 bp
Nest #1 reverse primer	ctgagtagctgggactac	51.2	
Nest #2 forward primer	acggagtctcactctgtc	53.2	1452 bp
Nest #2 reverse primer	caagctgtactctctggg	52	
Target Site 3			
Nest #1 forward primer	ggataaggcctaattccttgg	52.9	1618 bp
Nest #1 reverse primer	ggtaaccatccttctatgctc	52.5	
Nest #2 forward primer	gtcacctgctatttctctcc	52.5	1402 bp
Nest #2 reverse primer	gacacaagttgcttccag	51.1	
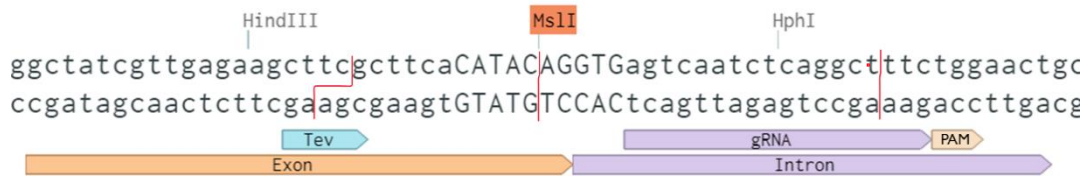
Figure 2.2. *Msl*I cut site for the cleavage resistance assay. The *Msl*I cut site is in capitalized letters. It spans the end of exon 10 and extends 3 bp into the intron.

2.10 T7 Endonuclease I Assay

T7 Endonuclease I (T7E1) assay was conducted following the extraction of genomic DNA from a population of transfected cells and PCR amplification of the target site. T7E1 (New England BioLabs Inc.) was used for this assay. First, an annealing reaction was set up composed of 200 ng of PCR-amplified DNA, 2 ul of NEBuffer 2 and water for a final reaction volume of 19 uL. This solution was heated in a thermocycler at 95°C for 5 minutes, then cooled at the rate of 2°C/second to 85°C, and finally cooled at the rate of 0.1°C/second to 25°C. T7E1 was then added (1 µL) to the annealed PCR products and incubated at 37°C for 15 minutes. T7E1, which indicates editing, was visualized by running the reaction on an agarose gel.

2.11 Target Locus Analysis

Tracking of Indels by DEcomposition (TIDE) is a webtool to assess genome editing at a target locus by CRIPSR-Cas9 (64). Analysis required the sequence of the gRNA, an electropherogram from Sanger sequencing reactions of the CRISPR-treated PCR-amplified target site, and an electropherogram from a control PCR-amplified target site. Using sequencing data, TIDE identified editing efficacy and the predominant types of insertions and deletions at the tested target site.

2.12 Western Blotting

Western blotting of protein was performed following the protocol outlined by Mahmood and Yang, 2012 with the following exceptions (65). A Bradford protein assay was used to quantify protein concentration (66). A sample of 10-35 µg of protein was loaded for each protein sample analysed. The Bio-Rad Trans-Blot Turbo transfer system, a semi-dry transfer method (Bio-Rad Laboratories, Inc.), was used to transfer protein from gel to a polyvinylidene fluoride membrane. Transfers were conducted at 2.5 amperes and 25 volts for 25 minutes.

Following transfer, the blot was blocked for 1 hour in 5% non-fat dry milk powder (Carnation®) prepared in Tris-buffered saline with Tween-20 (TBS-T; 50 mM Tris-Cl pH 8, 150 mM NaCl and 0.05% Tween-20) and incubated with primary antibodies diluted in

5% milk in TBS-T for 1 hour at room temperature or at 4°C overnight. After incubation, the blot was washed three times in a TBS-T solution before it was incubated with secondary antibody dissolved in 5% milk powder in TBS-T. The antibody complex was visualized using Clarity Western ECL Blotting Substrates (Bio-Rad Laboratories Inc.) and imaged using a ChemiDoc MP (Bio-Rad Laboratories Inc.). Images were analysed using Image Lab software (Bio-Rad Laboratories Inc.).

2.13 Immunofluorescence

Cells were seeded onto coverslips and incubated overnight. Cells were washed three times in phosphate-buffered saline (PBS; 137 mM NaCl, 10 mM phosphate, 2.7 mM KCl, and pH 7.4) and fixed on coverslips using 4% paraformaldehyde (BioShop Canada Inc.) for 15 minutes at 4°C. Coverslips were washed three times with PBS and cells were permeabilized using 0.5% Triton X-100 (BioShop Canada Inc.) for 15 minutes, followed by three washes with PBS. Coverslips were blocked in 5% FBS (Wisent Inc.) diluted in PBS for 1 hour at room temperature.

Coverslips were incubated overnight at 4°C with agitation in primary antibody diluted in 5% FBS (Wisent Inc.). Coverslips were washed three times with PBS then incubated with AlexaFluor 488 anti-mouse secondary antibody (Invitrogen Canada Inc.) for 1 hour at room temperature in the dark. Cells were washed three times with PBS then mounted on glass slides using ProLong® Gold antifade with 4′,6-diamidino-2-phenylindole (DAPI; Invitrogen Canada Inc.). Slides were imaged using an Olympus BX51 microscope (Olympus Corporation) and Image-Pro Plus software (Media Cybernetics Inc.). Images were analysed with ImageJ.

2.14 Antibodies

Primary antibodies used were Ku70 (N3H10; Santa Cruz Biotechnology, Inc.), Ku80 (M20; Santa Cruz Biotechnology, Inc.), Human influenza hemagglutinin for western blotting (H3663; Santa Cruz Biotechnology, Inc.), HA for immunofluorescence (H9658; Santa Cruz Biotechnology, Inc.), β-Actin (A5414; Sigma-Aldrich), Vinculin (E1E9V;

Cell Signaling Technology), and α-Tubulin (T5168; Sigma-Aldrich). Antibody
concentrations can be found in Table 3.

2.15 Statistical Analysis

Error bars indicating standard error of the mean are present on bar graphs. T-tests and
error bar calculations were completed on GraphPad (GraphPad Software Inc.). Analysis
by t-test resulting in a p-value of less than 0.001 conferred significance.

Table 2.3. Primary antibodies, their respective dilutions, and company

Antibody	Article number	Dilution	Company
HA [Western Blot]	H3663	1:1000	Santa Cruz
HA [Immunofluorescence]	H9658	1:1000	Sigma-Aldrich
Ku70	N3H10	1:1000	Santa Cruz
Ku80	M20	1:200	Santa Cruz
β-Actin	A5414	1:20000	Sigma-Aldrich
α-Tubulin	T5168	1:10000	Sigma-Aldrich
Vinculin	E1E9V	1:10000	Cell Signaling

Chapter 3

3   Results

3.1   Overview

Previous studies suggest that the evolutionarily conserved Ku heterodimer may be essential in human cells (39–41). Thus far, viable Ku knockout cell lines have only been successfully created in mouse cell lines and mice (17).

Since Ku exists and functions as an obligate heterodimer, targeting one subunit of Ku results in diminished expression of the other subunit (19, 67). Ku knockout studies have been conducted in a human colon cancer cell line, HCT116 by targeting both Ku70 and Ku80 independently (39, 40, 68). They found that heterozygous knockouts were viable but homozygous knockouts were not viable, implying that Ku80 and Ku70 were essential proteins in humans. We believe that further knockout studies would be valuable, particularly using other non-cancerous cell lines such as HEK293 cells and RPE1 cells. The goal of this project was to evaluate whether the knockout of Ku70 is lethal in human cells and to generate Ku70 knockouts to be used as a tool to further study the role of Ku in human cells. The tool we will be using to make these knockouts is a popular genome editing tool CRISPR/Cas9 system and the dual nuclease variation, CRISPR/TevCas9 system.

3.2   Attempt to Knockout Ku70 in WT Hek293 Cells

Ku70 knockouts were initially attempted in WT HEK293 cells. Preliminary experiments using live fluorescence imaging and cleavage resistance assays were conducted in WT HEK293 cells and the results suggested that TevSpCas9 and SpCas9 were expressing and cleaving *in vivo* (Figure 3.1). WT HEK293 cells were initially transfected with px458 plasmid carrying TevSpCas9 or SpCas9. Live-cell imaging revealed that TevCas9 was being transfected at higher levels compared to SpCas9 and no-gRNA plasmid transfection efficiency was lower than the gRNA-containing counterpart (Figure 3.1B). PCR-amplified product of target site 0 (Table 2.1) from genomic DNA extracted from transfected cells was digested with *Msl*I. Digestion was expected to produce 2 fragments,

685 bp and 285 bp in length. Resistance to cleavage would indicate that the *Msl*I site, located within the SpCas9/TevSpCas9 target site has been removed (Figure 2.2). Faint resistance bands were visualized on the cleavage resistance assay suggesting that TevSpCas9 and SpCas9 were cleaving *in vivo* (Figure 3.1A).

The transfected cell population was selected with puromycin for 5 days, after which puromycin was removed. Colonies were grown, then picked and cultured as monoclonal cell lines. Monoclonal cell lines were screened through western blotting (Figure 3.2). A total of 22 monoclonal cell lines were screened, and none of the cell lines showed decreased or abolished expression of Ku70 indicating that none of the clones were Ku70 knockdowns or knockouts.

Compared to the SpCas9 transfected cells, there was 2- to 3-fold greater cell death in the TevSpCas9 transfected cells (data not shown). Control cells transfected with SpCas9 and TevSpCas9 without gRNA died completely under antibiotic selection (data not shown).

3.3 Attempt to Knockout Ku70 in HEK293 Ku70-HA Stable Cells

We created a HEK293 stable cell line with an inducible second, exogenous copy of Ku70 controlled by a tetracycline-off (Tet-OFF) promoter. HEK293 cells were transfected with pBIG2r Ku70-HA constructs. Using hygromycin selection, a polyclonal HEK293 Ku70-HA cell line was created. To determine if and to what percentage the polyclonal stable cell line had integrated Ku70-HA, immunofluorescence was conducted with an HA antibody (Figure 3.3A). The immunofluorescence indicated that over 90% of the cells expressed Ku70-HA.

pBIG2R is a Tet-OFF system therefore gene expression of Ku70-HA in these cells can be shut off by the addition of either tetracycline or doxycycline. First, we confirmed that the Ku70-HA Tet-OFF system was functioning (Figure 3.3B, 3.3C). The addition of tetracycline for 5 days resulted in a decrease but not a complete shutdown of Ku70-HA expression (Figure 3.3B). Reduction in Ku70-HA did not appear to have a substantial effect on total Ku70 levels. Total Ku70 levels resembled the levels of the loading control,

A

B
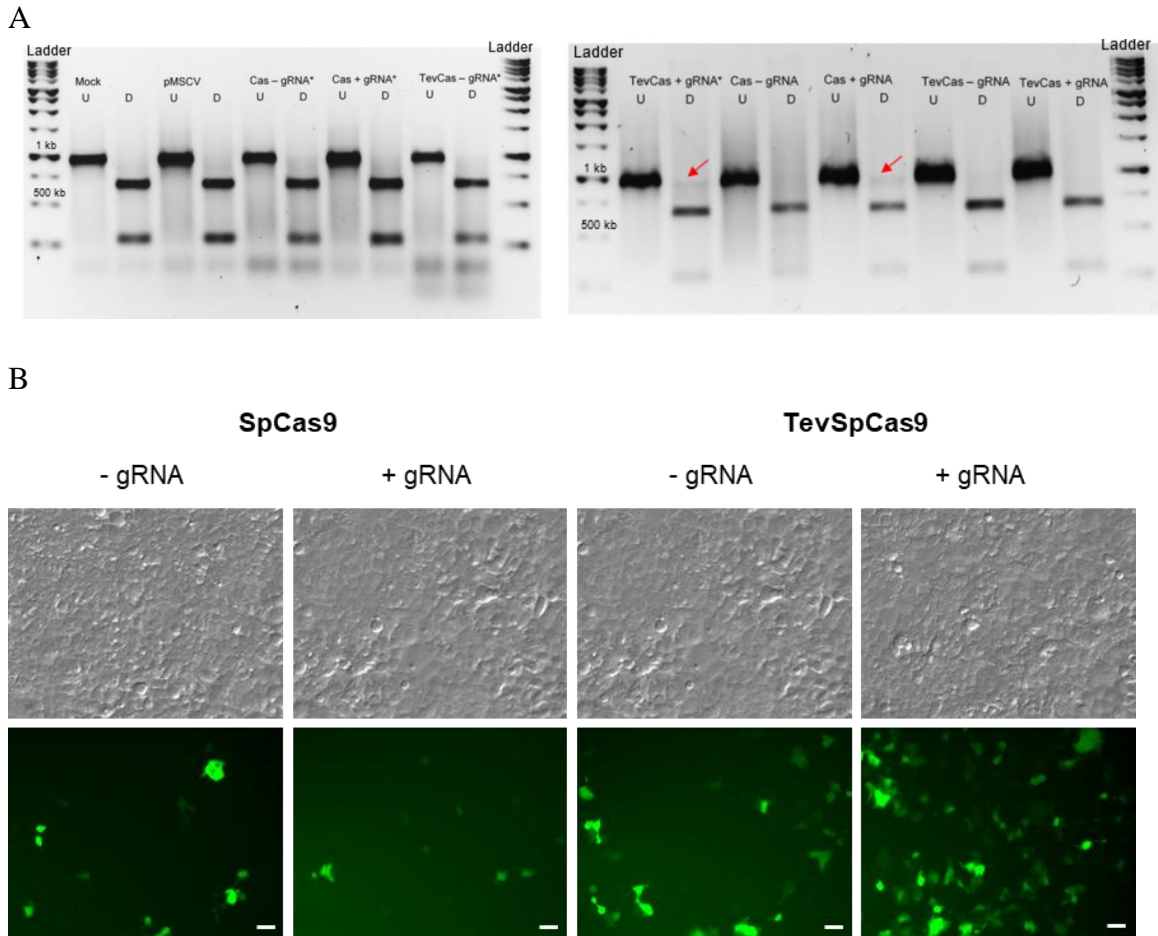
Figure 3.1A. Cleavage resistance assay to detect genome editing in regular HEK293 cells. TevCas9 and Cas9 with and without gRNA were transfected into HEK293 cells. Transfected cell populations were harvested 24 hours after transfection. Harvested samples were mock (no DNA was transfected), pMSCV$_{puro}$ (control vector without CRISPR was transfected), Cas9 – gRNA (no-gRNA), Cas9 + gRNA (with gRNA), TevCas9 – gRNA (no-gRNA), TevCas9 + gRNA (with gRNA). (*) indicated DNA harvested from separate transfections. DNA was extracted and amplified using nested PCRs and digested with *Msl*I. Undigested (U) and *Msl*I-digested (D) samples were run on a 1.5% agarose gel for 50 minutes at 90 V. Red arrows indicate the band suggesting resistance to *Msl*I cleavage. **B. Live fluorescence and contrast imaging of GFP-tagged SpCas9 and TevSpCas9 transfected HEK293 cells.** Visualized 24 hours after transfection. Top pane: HEK293 population under white light. Bottom pane: Visualization of GFP under blue light (488 nm) indicating nuclease expression. White bars denote 50 μm.
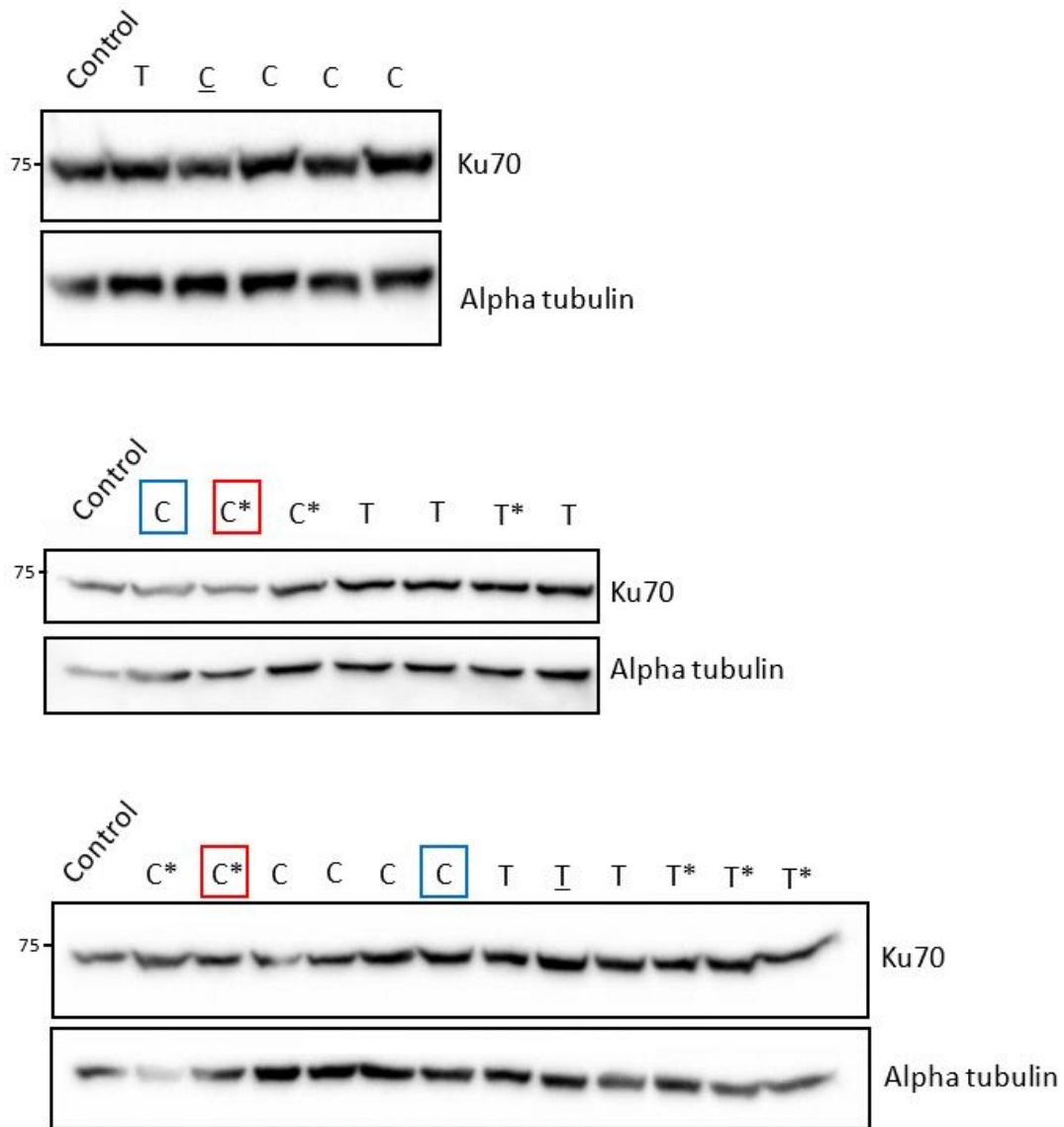
Figure 3.2: Western blot probing for Ku70 expression in HEK293 monoclonal cell lines. Samples were taken from SpCas9 (C) or TevSpCas9 (T) monoclonal cell lines or pooled cells. 20 monoclonal samples and 2 samples from entire populations were analysed. The blot was probed with anti-Ku70 and anti-alpha tubulin antibodies. Tubulin was used as a loading control. Underlined samples were extracted from a population and are not monoclonal cell lines. The red and blue squares indicated samples run twice on western blots. (*) indicated monoclonal cell lines isolated from co-transfection of px458SpCas9GFP (carrying the nuclease) and pMSCV$_{puro}$ (carrying puromycin resistance).

Actin (Figure 3.3B). This repression experiment was repeated using the antibiotic, doxycycline, which was kept on cells for 7 days instead of 5 days (Figure 3.3C). This resulted in better repression and very little expression of Ku70-HA after 7 days. This confirmed that we had a HEK293 cell line with Ku70-HA stably integrated under an inducible Tet-OFF promoter.

All further CRISPR experiments were conducted using px458$_{neoR}$SaCas9$_{GFP}$ and px458$_{neoR}$TevSaCas9$_{GFP}$ constructs. Both SaCas9 and TevSaCas9 in these constructs were T2A linked to GFP. T2A linker encodes a short DNA sequence that is translated into a self-cleaving peptide. The nuclease (SaCas9 or TevSaCas9) and GFP are transcribed on one mRNA. However, after translation, the linker will self-cleave and separate the nuclease and GFP into separate proteins. Live-cell imaging was used to detect protein expression of GFP and indirectly, of SaCas9 and TevSaCas9, 24 hours after transfection. The presence of GFP in these cells indicated that SaCas9 and TevSaCas9 were transfected and expressed in HEK293 Ku70-HA cells (Figure 3.4). Following transfection, these cells were selected with G418 antibiotic to select for cells containing px458$_{neoR}$SaCas9$_{GFP}$ or px458$_{neoR}$TevSaCas9$_{GFP}$ plasmids and monoclonal colonies were subsequently isolated and analysed.

SaCas9 and TevSaCas9 were transfected into these cells and monoclonal colonies were isolated and analysed. Out of over 40 analysed clones, two clones showed the highest reduction of Ku70 by Western blotting, clones 22 and 27 (Figure 3.5). When analysed genomically through sequencing, these clones showed heterozygous mutations that extended into the exon and disrupted the Ku70 splice site. Clone 22 contained a 54 bp heterozygous deletion, and clone 27 contained a 19 bp heterozygous deletion (Table 3.1). No growth defects such as abnormal cell morphology or change in cell growth rate were observed.
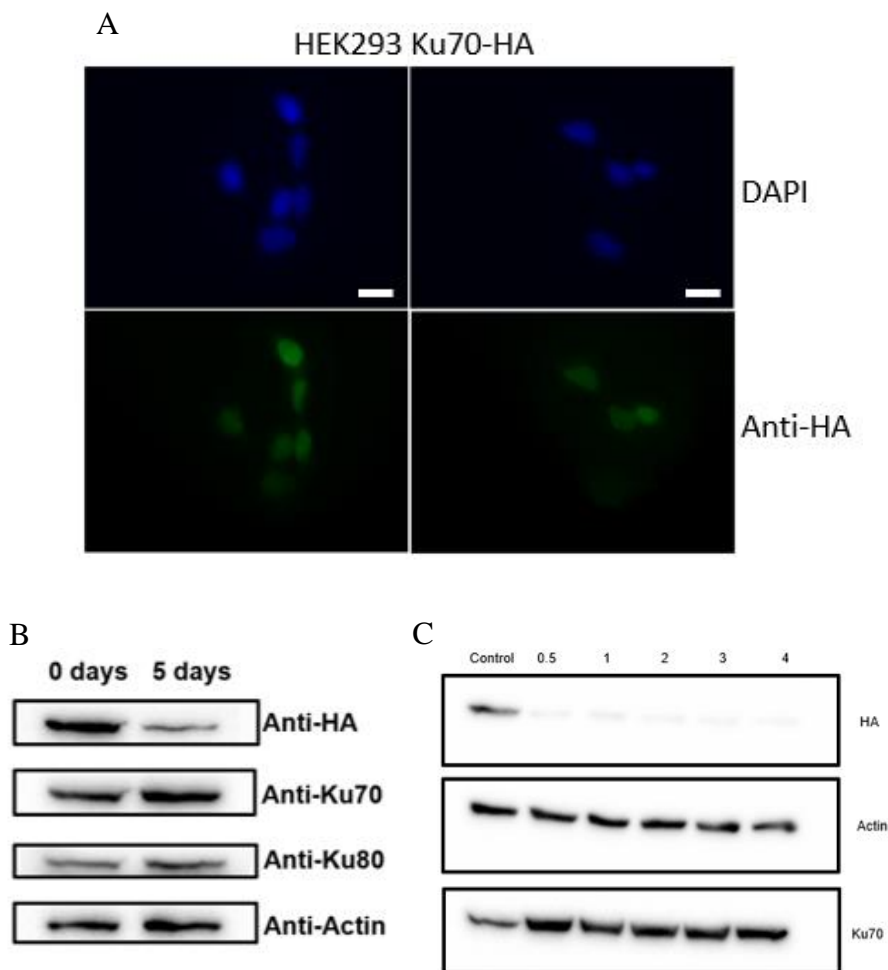
Figure 3.3A. Immunofluorescence probing for Ku70-HA expression in HEK293 Ku70-HA stable cells. Expression and cellular localization of Ku70-HA were visualized using immunofluorescence of HEK293 Ku70-HA cells stained with DAPI (blue) and probed with anti-HA antibody (green). White bars denote 50 μm. **B. Western blot analyses of tetracycline-induced repression of Ku70-HA in HEK293 Ku70-HA stable cells.** Whole cell extracts taken from HEK293 Ku70-HA cells that were treated with tetracycline (6 μg/mL) for 0 days and 5 days. Blot was probed with anti-Ku70, anti-Ku80, anti-HA and anti-actin antibodies. **C. Western blot analyses of doxycycline-induced repression of Ku70-HA in HEK293 Ku70-HA stable cells.** Whole cell extracts taken from HEK293 Ku70-HA cells that were treated with doxycycline (0.5, 1, 2, 3, and 4 μg/mL) for 7 days. Blot was probed with anti-Ku70, anti-HA and anti-actin antibodies.
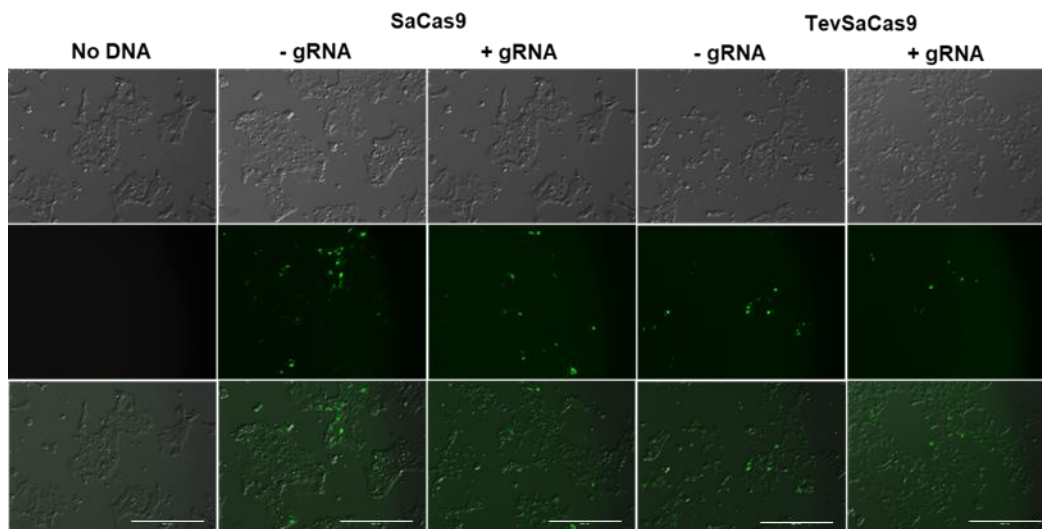
Figure 3.4. Fluorescence and contrast imaging to visualize transfection efficiency in HEK293 Ku70-HA cells. Cells were transfected with no DNA, SaCas9-GFP (with and without gRNA), and TevSaCas9-GFP (with and without gRNA) containing plasmids and visualized 24 hours after transfection. The top row shows HEK293 population under white light. The middle row shows the visualization of GFP excited under blue light (488 nm) indicating nuclease expression in fluorescing cells. The bottom row is the top two rows overlaid to show the position of cells relative to the position of fluorescence. White bars denote 1000 μm.

A
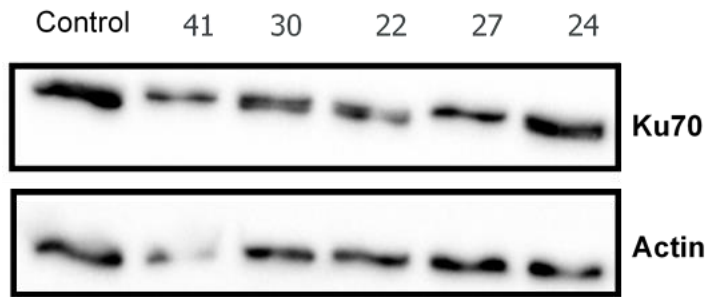
B
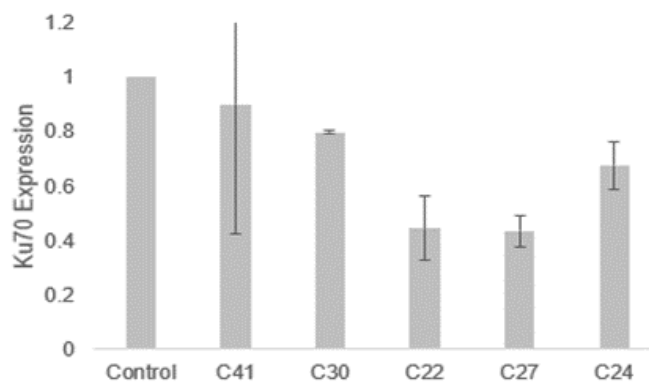
Figure 3.5A. Western blot analyses of Ku70 expression in SaCas9 transfection-derived HEK293 Ku70-HA monoclonal cell lines. Whole cell extracts taken from monoclonal HEK293 Ku70-HA cells transfected with SaCas9 and selected with G418. Blot was probed with anti-Ku70 and anti-actin antibodies. **B. Quantitative analyses of Ku70 levels in SaCas9 transfection-derived HEK293 Ku70-HA stable cells.** Ku70 levels in SaCas9 transfection-derived HEK293 Ku70-HA monoclonal cell lines were quantified compared to WT HEK293 Ku70-HA control and averaged for each clone (n=3).

Table 3.1. Genetic analyses of HEK293 Ku70-HA monoclonal cell lines after CRISPR treatment. Monoclonal cell lines were picked from CRISPR-transfected HEK293 Ku70-HA cells after G418 selection. The gRNA targeted site was PCR-amplified and sequenced. Electropherograms were analysed manually and using TIDE to determine the size of the editing event and if the editing affected the intron-exon splice site. The table shows the genetic analyses of all clones that showed editing events.

Clone #	Types of editing	Effects splice site?
1	140 bp insertion	No
2	19 bp insertion, 41 bp insertion	No
3	11 bp deletion, 2 bp deletion, 19 bp insertion	Yes
4	>50 bp insertions (2)	No
5	7 bp deletion	No
6	2 bp insertion, 3 bp insertion, >50 bp insertion	No
10	239 bp deletion	No
16	73 bp insertion, 97 bp insertion	No
18	140 bp insertion	No
19	28 bp deletion, 1 bp insertion, 18 bp deletion	Yes
22*	54 bp deletion	Yes
23	400 bp insertion from chromosome 19	No
27*	19 bp deletion	Yes

3.4   Ku70 Gene Editing in RPE1 Cells

Experiments were halted in HEK293 Ku70-HA cells and switched to RPE1 cells for several reasons. The HEK293 Ku70-HA clones became contaminated with fungi and could not be used in experiments any further. Additionally, some of the sequencing electropherograms of the HEK293 Ku70-HA clones contained more than two signals. This indicated that HEK293 cells carries more than two copies of the gene that encodes Ku70. Literature searches confirmed that HEK293 cells are tetraploid for chromosome 22, the chromosome that carries the Ku70 gene (44). RPE1 cells are a near-diploid cell line (45) which we believe may better mimic 'normal' human cells compared to polyploid cell lines such as HEK293. This would help generalize results from immortal cells to normal human cells.

First, Ku70 levels in RPE1 and HEK293 cells were compared. As expected from the respective Ku70 gene copy number, we found that RPE1 cells had significantly less Ku70 levels (Figure 3.6). Preliminary transfections were conducted to optimize transfection efficiency in RPE1. RPE1 cells on average had lower transfection efficiency compared to HEK293 cells. We found that by using Lipofectamine 3000 (Thermo Fisher Scientific Inc.) we were able to get 10 to 20% transfection efficiency (Figure 3.7).

Ku70 CRISPR knockouts were attempted in WT RPE1 cells. Interestingly, 24 hours after CRISPR transfection, cells transfected with gRNA showed more death in comparison to cells transfected with no-gRNA as control (Figure 3.8).

RPE1 cells transfected with SaCas9 or TevSaCas9 with Ku70 targeting gRNA were also harvested 24 hours after transfection. Genomic DNA was extracted from the cell population and target site 1 was PCR-amplified using nested PCRs. The PCR product was sequenced and analysed using TIDE to determine the amount of editing present and most common insertion or deletion events. In the SaCas9 transfected population, the total editing efficiency was found to be 2.2%, with the most common editing event being a 1 bp insertion event. In the TevSaCas9 transfected population, the total editing efficiency was calculated as 8.7%, with the most common editing event being a 36 bp deletion (Figure 3.9).

A

B
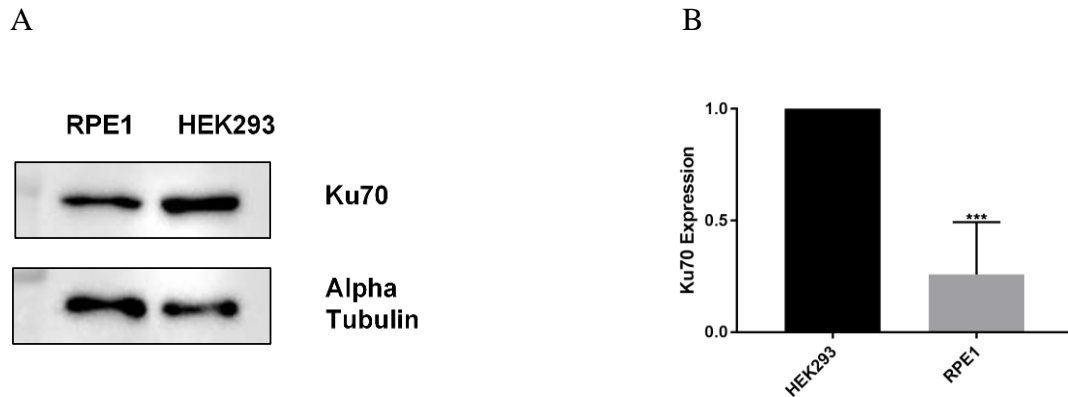
Figure 3.6A. Western blot analyses of Ku70 levels in RPE1 cells and HEK293.
Whole cell extracts from WT RPE1 and HEK293 were analysed using sodium dodecyl
sulfate-polyacrylamide gel electrophoresis (SDS-PAGE). Blot was probed with anti-
Ku70 and anti-alpha tubulin antibodies as loading control. **B.** Quantitative analyses of
Ku70 levels in RPE1 cells and HEK293. Ku70 levels in WT RPE1 cell were quantified
compared to WT HEK293 control and averaged for each cell line (n=3) (*** $p<0.001$).
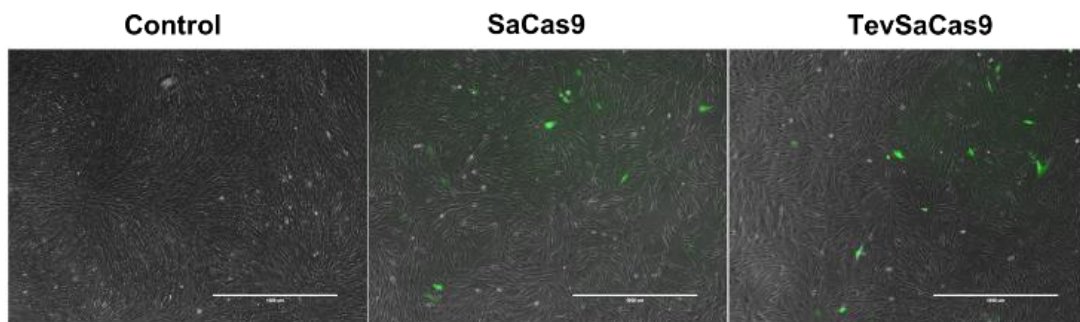
**Figure 3.7. Overlay of live-cell fluorescence and contrast imaging to visualize
transfection efficiency in RPE1 cells.** RPE1 cells were transfected with no DNA,
SaCas9-GFP, and TevSaCas9-GFP containing plasmids. 24 hours after lipofectamine
transfection RPE1 population was visualized under white light (contrast imaging) and
blue light (488 nm; GFP fluorescence imaging) and images were overlaid. Presence of
GFP fluorescence indicated nuclease expression in cells. White bars denote 1000 μm.
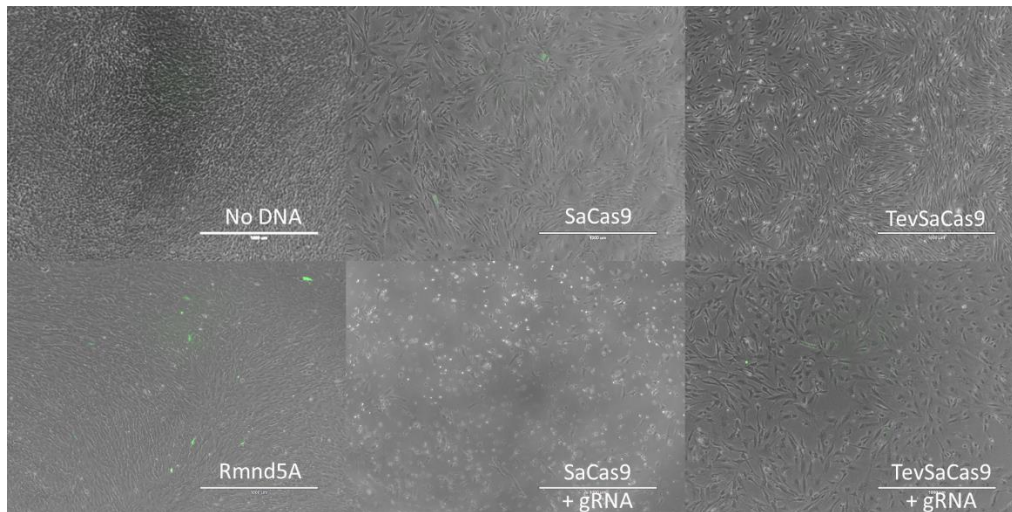
Figure 3.8. Overlay of fluorescence and contrast imaging visualizing transfection efficiency and confluency of RPE1 cells. Samples were transfected with no DNA, SaCas9-GFP + Rmnd5A gRNA, SaCas9-GFP no-gRNA, SaCas9-GFP + Ku70 gRNA, TevSaCas9-GFP, and TevSaCas9-GFP + Ku70 gRNA-containing plasmids. RPE1 population under white light and blue light (488 nm) was visualized 24 hours after jetPRIME transfection and images were overlaid. GFP fluorescence indicated nuclease expression in fluorescing cells. White bars denote 1000 μm.

Figure 3.9. TIDE analyses of gene editing events in SaCas9 and TevSaCas9 transfected RPE1 cells. 24 hours after transfection, population of SaCas9 or TevSaCas9 transfected RPE1 cells were harvested and DNA was extracted. The gRNA targeted site was PCR-amplified and sequenced. Electropherograms were analysed using TIDE to determine the size of common editing events in each population.

RPE1 cells transfected with SaCas9 and TevSaCas9 with Ku70 targeting gRNA were selected with G418 for 7 days. G418 was removed and colonies are grown and picked. A total of 45 clones, picked from two separate transfections, were screened. Figure 10A shows Ku70 expression of a portion of clones. None of the clones screened completely lacked Ku70 expression but some clones appeared to have decreased Ku70 levels. However, when further screening was conducted using T7 endonuclease I assays, no genome editing was found (Figure 3.10B). Multiple attempts were made to create RPE1 Ku70-HA stable cells, however, none were successful.

3.5   HEK293 TREX Ku70-HA Cells

While attempting to create the inducible Ku70-HA system in RPE1 cells, I also recreated HEK293 Ku70-HA stable cells in parallel, as previous research in HEK293 Ku70 was disrupted due to fungal contamination.

I was able to generate HEK293 TREX TET-ON Ku70-HA stable cells. The HEK293 TREX cell line constitutively expresses the tetracycline repressor. Cells were transfected with a plasmid carrying Ku70-HA under control of a tetracycline operon. In the absence of tetracycline (or doxycycline), the tetracycline repressor protein bound to the operon and repressed transcription of Ku70-HA. If tetracycline or doxycycline antibiotics were added, they bound the tetracycline repressor and did not allow it to block transcription of the promoter, thus inducing expression of Ku70-HA.

This stable cell line was created using a different inducible system compared to previously. The initial HEK293 Ku70-HA stable cells used a TET-OFF system and were polyclonal with over 90% of cells showing Ku70-HA expression. HEK293 TREX Ku70-HA stable cells were a tetracycline-ON (TET-ON) system and isogenic polyclonal with 100% of cells showing Ku70-HA expression as visualized by immunofluorescence (Figure 3.11).

A

B
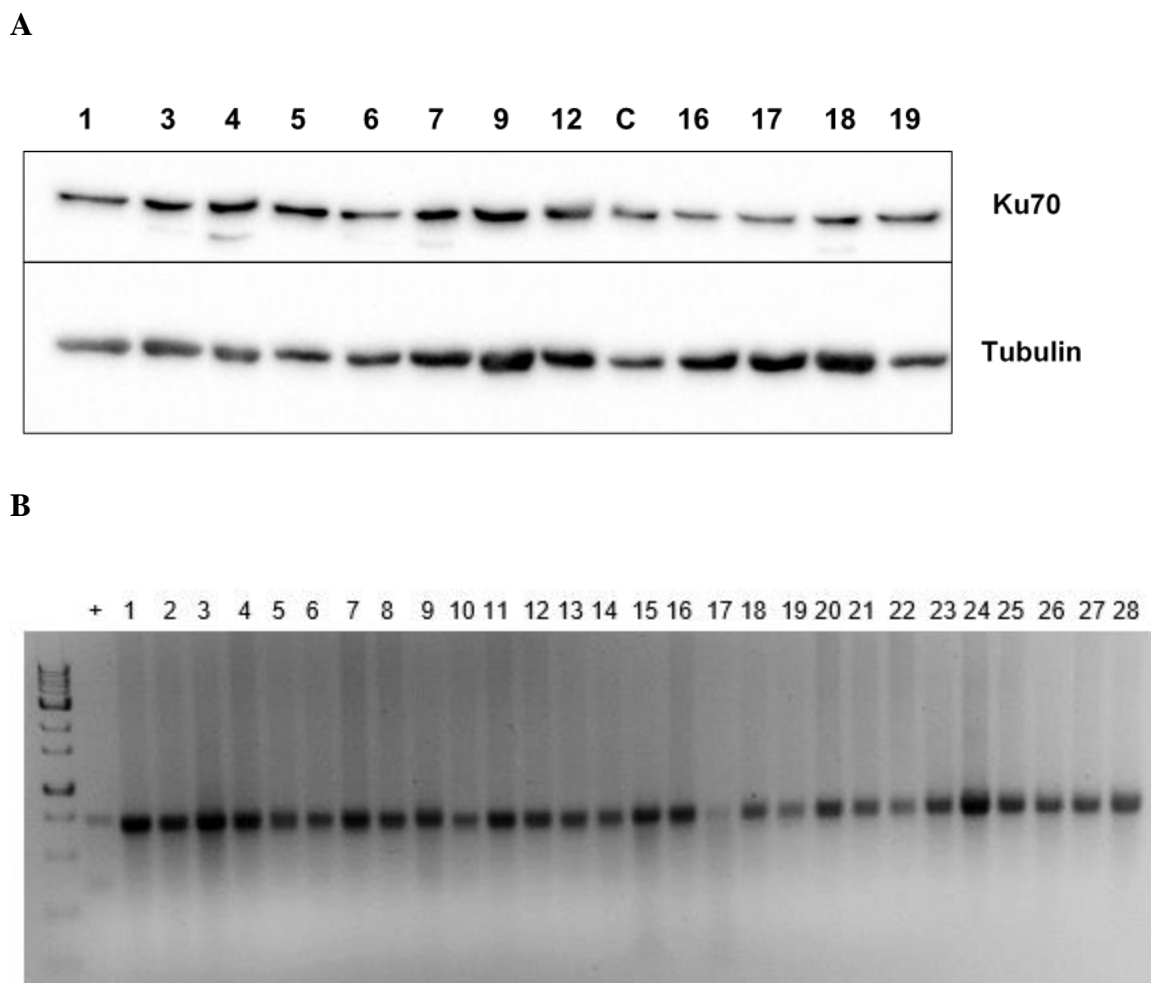
Figure 3.10A. Western blot analyses of Ku70 levels in CRISPR RPE1 cells monoclonal cell lines. Whole cell extracts from RPE1 CRISPR monoclonal cell lines were analysed using SDS-PAGE. Blot was probed with anti-Ku70 antibody and anti-alpha tubulin antibody as a loading control. **B. Agarose gel showing T7EI assay to detect genome editing in RPE1 CRISPR monoclonal cell lines.** DNA was extracted from RPE1 CRISPR monoclonal cell lines and that gRNA targeted region was amplified using PCR. T7 endonuclease assay was performed with WT RPE1 DNA and monoclonal cell DNA and run on an agarose gel.
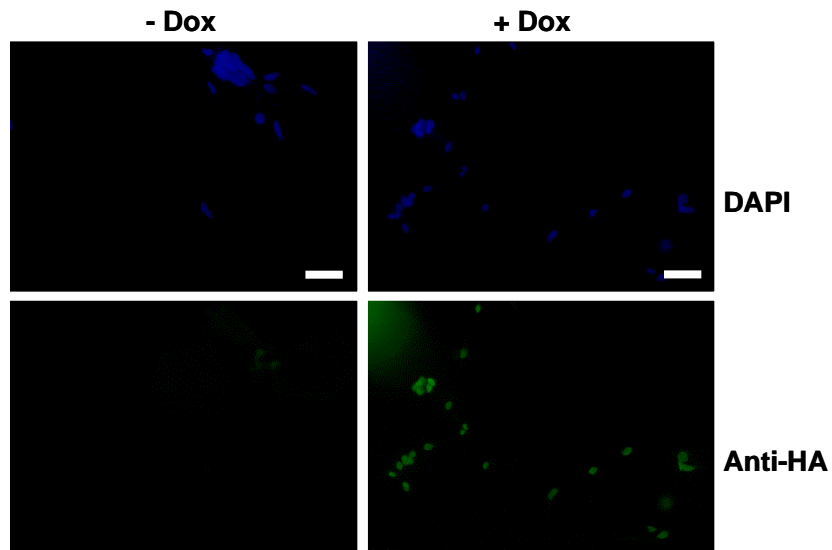
Figure 3.11. Immunofluorescence visualizing Ku70-HA in HEK293 Ku70-HA TREX stable cells induced and uninduced with doxycycline. Ku70-HA expression was induced with doxycycline for 24 hours. Cells were probed with DAPI (blue) and anti-HA antibodies (green). White bars denote 200 μm.

Next, the Ku70-HA TET-ON system was characterized. After the addition of doxycycline, 8 hours was the shortest timepoint at which Ku70-HA was detected by western blot and 16 hours appeared to represent the timepoint for maximum Ku70-HA expression (Figure 3.12A). After the removal of doxycycline, it took at least seven days for the near-complete disappearance of Ku70-HA (Figure 3.12B). Total Ku70 levels appear to correlate to tubulin levels and were not affected by the reduction of Ku70-HA, indicating that Ku70-HA levels do not make up a substantial proportion of total Ku70 in the cells.

This new HEK293 TREX Ku70-HA cell line was consistently cultured in 1 µg/ml of doxycycline to express back-up Ku70-HA and transfected with SaCas9 and TevSaCas9 containing plasmids. For these experiments, three separate gRNA targeting three different intron-exon junctions in Ku70 (exon 6, 7, and 12) were selected. They were cloned using golden gate into individual px458$_{neoR}$SaCas9$_{GFP}$ and px458$_{neoR}$TevSaCas9$_{GFP}$ plasmids. During transfection, cells were co-transfected with either three px458$_{neoR}$SaCas9$_{GFP}$ constructs or three px458$_{neoR}$TevSaCas9$_{GFP}$, each containing one of three gRNA.

Over 60 clones were isolated from SaCas9 and TevSaCas9 transfected HEK293 TREX Ku70-HA cells. Select clones were analysed through Western blotting for protein analysis by graduate student, Rachel Kelly (Figure 3.13). Three potential knockout candidates were found, Sa11, TIA, and SA. These clones showed substantially lowered expression of both Ku70 and Ku80 when doxycycline was removed for 9 days from their media leading to the shut off of Ku70-HA expression.
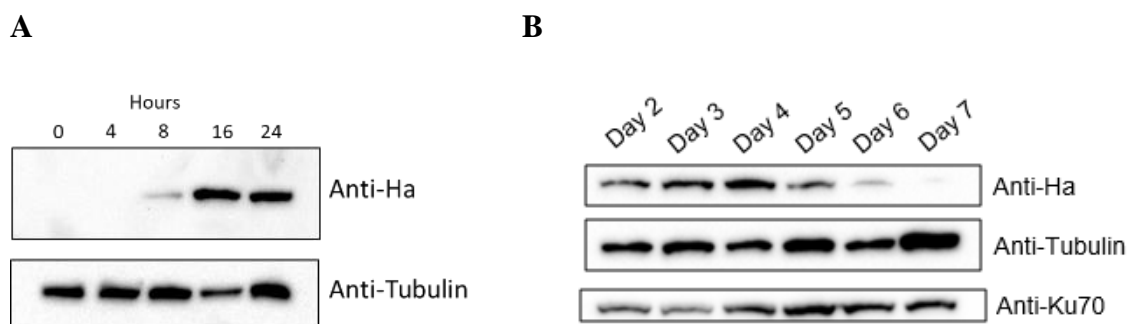
Figure 3.12A. Western blot analyses of doxycycline-induced expression of Ku70-HA in HEK293 Ku70-HA TREX stable cells. Whole cell extracts taken from HEK293 Ku70-HA TREX cells that were treated with doxycycline (1 µg/ml) for 0, 4, 8, 16, 24 hours. Blot was probed with, anti-HA and anti-actin antibodies. **B. Western blot analyses of repression of Ku70-HA in HEK293 Ku70-HA TREX stable cells in the absence of doxycycline.** Whole cell extracts taken from HEK293 Ku70-HA TREX cells that were treated with doxycycline (1 µg/ml) for 24 hours. Afterwards, doxycycline was removed and cells were harvested at different timepoints (2 – 7 days). Blot was probed with anti-Ku70, anti-HA and anti-actin antibodies.

A
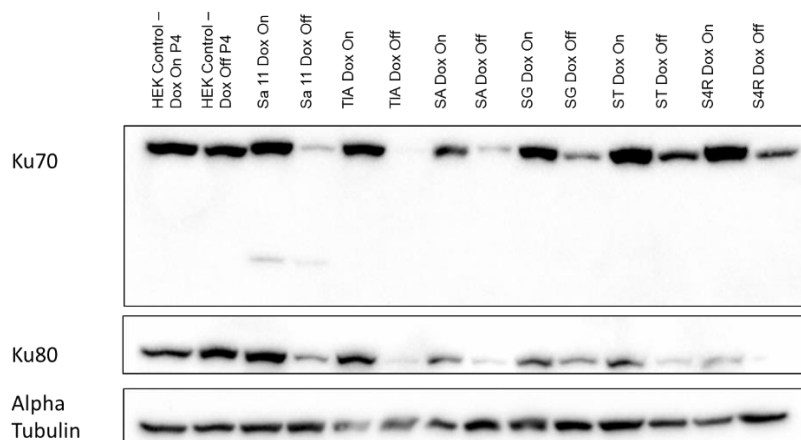
B
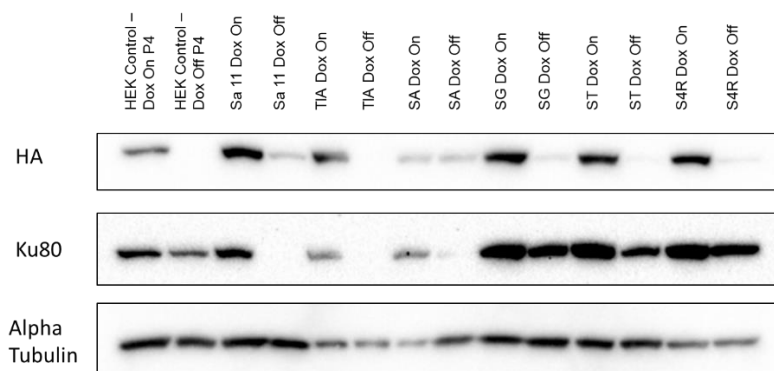
Figure 3.13A. Western blot analyses of SaCas9 and TevCas9 treated HEK293 Ku70-HA monoclonal cell lines. Cell harvesting and Western blotting was conducted by graduate student, Rachel Kelly. Whole cell extracts taken from monoclonal cell lines picked from CRISPR-transfected HEK293 Ku70-HA cells selected with G418. Doxycycline was removed from Dox off samples for 9 days prior to harvest and lysis. Blot was probed with anti-Ku70 antibody, anti-Ku80 antibody and anti-tubulin antibody as the loading control. **B. Western blot analyses of the same SaCas9 and TevCas9 treated HEK293 Ku70-HA monoclonal cell lines from Figure 3.13A.** Cell harvesting, and Western blotting was conducted by graduate student, Rachel Kelly. Whole cell extracts taken from monoclonal cell lines from Figure 3.13A were run on a separate gel to probe specifically for Ku70-HA (not endogenous Ku70). Blot was probed with anti-HA antibody, anti-Ku80 antibody and anti-tubulin antibody as the loading control.

Chapter 4

4   Discussion

4.1   Summary

The objective of this project was to create Ku70 knockouts as a tool to study Ku mutants and to evaluate whether Ku70 is essential or not in human cells. The aim was also to compare knockout efficiencies of two gene editing tools, CRISPR/Cas9 and CRISPR/TevCas9 that were used to create Ku70 knockouts in HEK293 cells and RPE1 cells. We created stable cell lines with a second, inducible copy of Ku70-HA to attempt to create conditional knockouts of Ku70 to more definitively evaluate the effect that deleting Ku70 on human cells. We were unsuccessful in creating an inducible Ku70-HA system in RPE1 cells, possibly due to poor transfection efficiency. In HEK293 Ku70-HA cells, we were able to knockout Ku70, in the presence of Ku70-HA.

4.2   Knockout Attempts in WT HEK293 Cells

Experiments conducted in wild type HEK293 cells suggest that TevSpCas9 and SpCas9 were expressing and cleaving *in vivo*. Cleavage resistance assays performed using DNA harvested from TevSpCas9 and SpCas9 transfected cells indicated that the nucleases were active in HEK293 cells and genome editing was occurring. However, when monoclonal colonies were analysed, no knockouts were found. This may have been due to many factors. The first reason may be that too few clones were screened. Only 22 monoclonal cell lines were analysed. The resistance bands in the digested lane on the cleavage resistance assay were very faint compared to the band in the undigested lane, indicating that a very small

proportion of the cells in the population underwent editing. If the gRNA targeting efficiency was low or the plasmid transfection efficiency was low, this may have increased the number of clones that were required to be screened to identify a Ku70 knockout. Another reason may be that Ku70 is essential, as editing can be visualized in the cleavage resistance assay when cells were harvested only 24 hours after selection. However, after passaging cells in the process of culturing colonies into monoclonal cell lines, the Ku70 knockout cells may have died. Alternatively, some editing events may be isolated to the intronic region and have no effect on the final protein product. Since the *Msl*I restriction site spans the intron-exon junction, cleavage resistance likely indicates that the deletion extended into the exon. It is possible, however, that the deletion may not reach the exon and have no effect on the Ku70 protein. The cut site for *Msl*I extends 3 bp into the intron, and modification in those base pairs will disrupt the enzyme cut site and produce resistance to cleavage however, since it is located in the intron, will not affect Ku70 protein expression.

Interestingly, it was observed that compared to the SpCas9 transfected sample, there was 2- to 3-fold more cell death in the TevSpCas9 transfected sample. This is not due to poor TevSpCas9 transfection efficiency as live-cell imaging revealed that TevCas9 was being transfected at higher levels compared to SpCas9. One possible explanation for this could be that although TevSpCas9 is being successfully transfected, it may simply be more toxic to cells than Cas9. It remains to be further examined. This could be determined by comparing cell death between HEK293 cells transfected with control plasmids containing SpCas9 and TevSpCas9 but missing gRNA. However, conclusions about TevSpCas9 toxicity could not be made because following antibiotic selection, these controls displayed

complete cell death. It is unclear why cells transfected with no-gRNA control plasmids did not survive antibiotic selection. Live-cell imaging revealed that the no-gRNA transfection was successful however occurred at a lower efficiency than the Ku70 gRNA-containing counterpart. Lower transfection efficiency may have led to cell death following selection. However, further transfections are required to determine TevSpCas9 toxicity compared to SpCas9.

Another possibility is that TevSpCas9 may be more successfully inducing deletions in the Ku70 exon. If true, this would suggest that the successful knockout of Ku70 is lethal, and this could explain the difference in observed cell death between TevSpCas9 and SpCas9. This is supported by the observation that confluency differences were only in plates transfected with TevSpCas9 and SpCas9 with gRNA, not in plates transfected without gRNA. This would match the results of previous attempts at knocking down Ku that found knockout resulted in cell death (39–41). The SpCas9 cells may have survived because SpCas9 created heterogeneous indels that were largely located in the intron and do not extend into the preceding exon. However, there was not enough evidence to fully support this conclusion. This could be determined using Illumina sequencing of PCR-amplified product containing the target site used for the cleavage resistance assay.

Deep sequencing could be used to determine the type and length of indels as well as quantify the frequency of these editing events. This technique was previously used in Wolfs *et. al.* (2016) to show the 33-36 bp deletion bias caused by TevSpCas9 (53). When analysing target site DNA from SpCas9 transfected cells, a range of insertion and deletions lengths were observed, most common being a +1 insertion event (53). It appears that +1 insertion events are one of the most common editing events caused by SpCas9 (69). In my

experiments, editing events of a +1 insertion caused by SpCas9 targeting target site 0 would occur exclusively in the intron in the Ku70 gene and would not affect the protein sequence of Ku70. This may explain why less cell death was observed in SpCas9 transfected cells if we assumed that Ku70 is essential.

We followed up these experiments with the construction of a stable cell line with a second inducible copy of Ku70 with tetracycline-controlled transcriptional activation. If Ku70 can be successfully knocked out in these cells, this system can be used to investigate the lethality of a Ku70 knockout. If shutting off the expression of the second copy of Ku results in the death of the knockout cells, this will confirm that Ku is essential in HEK293 cells.

4.3   Analysing CRISPR Clones in HEK293 Ku70-HA Stable Cells

We created a HEK293 stable polyclonal cell line with an inducible second, exogenous copy of Ku70 controlled by a Tet-OFF promoter. Ku70-HA expression decreased in response to tetracycline. However, we found it preferable to use doxycycline instead. While both tetracycline and doxycycline have a half-life of approximately 24 hours in tissue culture media, lower concentrations of doxycycline can be used to produce the same induction effect as tetracycline used at a much higher, possibly cytotoxic level (70). Even after 7 days of doxycycline repression, the TET-OFF system still showed some very faint bands indicating very low levels of Ku70-HA expression on a western blot. This could be due to leakage of the TET-OFF system or incomplete degradation of Ku70. Ku70 may require longer than 7 days to be completely degraded.

CRISPR transfections were repeated in HEK293 Ku70-HA stable cells. Constructs containing SaCas9 and TevSaCas9 T2A linked to GFP were used hereafter in these experiments in the place of SpCas9 and TevSpCas9 containing constructs. Live-cell imaging confirmed successful transfection and expression of the nucleases in HEK293 Ku70-HA cells. Out of 40 analysed clones, 2 clones derived from SaCas9 transfected HEK293 Ku70-HA cells, clones 22 and 27, showed significant knockdown of Ku70 expression. After genome analysis, we determined that clone 22 showed a 54 bp heterozygous deletion while clone 27 contained a 19 bp heterozygous deletion. Both deletion events were large enough to extend into the exon which means that the deletions likely functioned to disrupt the splicing of Ku70. Interestingly, these mutations were heterozygous. It has been observed that heterozygous Ku70 HTC116 knockouts are haploinsufficient for Ku70 as they have slower growth rate, higher sensitivity to ionizing radiation, and shortened telomeres compared to wild type HTC116 (68). Similar phenotypes were also observed in heterozygous Ku80 knockouts (40, 71). Clones 22 and 27 were not tested for telomere length or ionizing radiation sensitivity, however, they did not display the slower growth rate phenotype.

It is important to note that these knockout experiments were conducted in HEK293 Ku70-HA cells which contained a backup copy of Ku70-HA. This extra copy could have allowed these heterozygous knockouts to overcome the haploinsufficiency. However, there was not enough data to conclude Ku70 haploinsufficiency in these clones. Unfortunately, due to fungal contamination, these clones were not analysed after doxycycline release to observe their behaviour and Ku70 expression levels after shutting off Ku70-HA expression. HEK293 are tetraploid for chromosome 22, the chromosome that carries the Ku70 gene

(72). This may be another possible reason why our heterozygous knockout clones did not show a growth rate defect.

4.4   Ku Levels in Human Cells

RPE1 cells were found to have significantly lower Ku70 expression compared to HEK293 cells. This is consistent with each cell line's respective gene copy number. Many common immortalized cell lines used in the lab show high levels of genomic instability and are polyploid for chromosome 22, such as HeLa and HEK293 cell lines (73, 74). In normal cells, Ku is most well-known for its function in NHEJ, however, it has also been implicated in V(D)J recombination, telomere conservation, DNA replication, cell cycle control and anti-apoptosis (17, 71, 72). Interestingly, Ku upregulation has been linked to the progression of certain tumour types, such as chronic lymphocytic leukemia, bladder cancer and breast cancer (75, 76). This may support our assumption that a near-diploid cell line such as RPE1 cells may be more representative of 'normal' human cells compared to polyploid cell lines such as HEK293 and cancer cell lines such as HTC116. Higher levels of Ku in cells more prone to genomic instability may indicate a higher dependence on Ku and its role in various cellular processes. Thus, knockout of Ku in these cells may only produce cell line specific results and may not be generalized to 'normal' human cells. This remains to be further explored by comparing Ku levels and attempting heterozygous and homozygous knockouts across various (primary, immortalized, stable diploid and cancerous) human cell lines.

4.5   CRISPR in RPE1 Cells

CRISPR experiments conducted in wild type RPE1 cells yielded interesting results. As seen in HEK293 Ku70-HA cells, live-cell imaging revealed that SaCas9 and TevSaCas9 were being transfected and expressed in RPE1 cells. Similar to observations made for transfections conducted in wild type HEK293 cells, RPE1 cells transfected with gRNA show more death in comparison to cells transfected with no-gRNA as control. This supports the suggestion that Ku70 knockouts are lethal. This hypothesis is also consistent with previously seen results observed in wild type HEK293 cells where TevSpCas9 + gRNA transfected samples showed higher cell death compared to SpCas9 + gRNA. TevSpCas9 may have been creating Ku70 knockouts more efficiently and killing more cells compared to SaCas9.

CRISPR-transfected RPE1 population before antibiotic selection were genomically analysed using TIDE to screen for editing events in the population after transfection. Very low levels of editing were found in both SaCas9 and TevSaCas9 samples. Interestingly, the most common editing event in the SaCas9 sample was a 1 bp insertion. This was expected and consistent with the fact that a 1 bp insertion is the most common indel created by Cas9 (69, 77). The TevSaCas9 sample revealed the most common editing event to be 36 base pair deletion. This was expected as it corresponds to the length of bases between the Tev cut site and the SaCas9 cut site present in the TevSaCas9 target site. This provided strong support that SaCas9 and TevSaCas9 were functional in RPE1 cells and at the Ku70 gRNA targeted site, however, this occurred at a very low level. Out of over 60 clones screened, no knockouts or knockout candidates were found. This was not surprising as

Ku70 appears to be a difficult gene to target for gene editing. Fattah *et. al.* (2008) found a success rate of 0.69% when attempting to target the Ku70 gene in HCT116 cells (68). They were only able to obtain 3 Ku70 heterozygous knockouts out of the screened 437 antibiotic-resistant clones. Interestingly, retargeting the remaining Ku70 allele in heterozygous knockouts resulted in a 6-fold increase in gene targeting frequency. From their results, it appears reduced Ku70 expression levels may increase the frequency of gene targeting. It is important to note that gene editing was accomplished through the use of recombinant adeno-associated virus which relies on homologous recombination (68). This differs from the method used in this project, SaCas9, which relies on NHEJ without the presence of a repair complex.

The answer may simply lie in the screening of more clones to acquire an RPE1 Ku70 knockout. A study in *Nature Medicine* reported that genome editing using CRISPR may be less efficient in human cells with a wild type p53 response such as RPE1 cells (78). Their results suggest in p53-proficient cells, Cas9 induced DSBs to activate p53, leading to a growth arrest. This explains the relative difficulty of editing normal, untransformed human cells.

4.6   Attempting to Create Ku70-HA Stable Cells in RPE1 Cells

Many unsuccessful attempts were made to recreate the inducible Ku70-HA system in RPE1 cells using many different transfection methods (Lipofectamine 3000, jetPRIME, Mirus Bio TransIT-X2, and calcium phosphate). Though all methods were able to successfully transiently transfect plasmid carrying tetracycline-controlled Ku70-HA into RPE1 cells, none resulted in stable integration after selection. It is unclear at this point what the problem

may be. Low RPE1 transfection efficiency may require more colonies to be screened when creating a stable cell line. Different methods of transfections should be tested to increase transfection efficiency. Fugene (79), liposome-mediated transfection method and Lonza Nucleofector, electroporation method, (80) have been successful in RPE1 cells.

4.7 CRISPR Clones in TREX HEK293 Ku70-HA Stable Cells

In the second attempt to obtain Ku70 knockout HEK293 cells, transfections were performed with 3 gRNAs, simultaneously targeting exon 6, 7, and 12, whereas previous experiments only used one gRNA. Over 60 monoclonal cell lines were screened with doxycycline and without doxycycline (for 8 days). Clones Sa11, SA (SaCas9 clones) and TIA (TevCas9 clone) cultured without doxycycline showed very low to no Ku70 expression. Ku80 showed the same result. This was expected as Ku70 and Ku80 are obligate heterodimers, meaning that the knockout of either subunit in Ku results in a drop in expression of the other to negligible levels. Subunit dimerization likely has a stabilizing effect on both subunits (18, 19). The absence of Ku80 further supports the conclusion that these clones are indeed Ku70 knockouts.

Efficiencies of SaCas9 compared to TevSaCas9 can be determined after analyses of 50+ clones that are yet to be screened. When comparing the number of clones, SaCas9 provided 3 - 4 times more clones compared to TevSaCas9 transfections. Part of this discrepancy may be explained by the fact that SaCas9 is about 2 kb smaller than TevCas9 and smaller plasmids usually have a higher transfection efficiency (81).

4.8   Future Perspective

In future studies, these clones will have to be analysed by sequencing to determine which gRNA caused an indel that disrupted the splice site of Ku70. It would be interesting to see if more than one gRNA target site showed editing. Doxycycline released cells need to be observed for cell death to determine whether Ku70 is essential in HEK293 cells. Our conditional knockout can also be used to study the stability of Ku70 in HEK293 cells by measuring the length of time required for complete Ku70 depletion after doxycycline release. Many other factors can also be observed such as any phenotype changes observed in the knockouts after doxycycline release and changes in telomere length of the knockouts once doxycycline is removed. Ku functions by promoting the association of telomerase with telomeres (30–32). It has been speculated that the essential function of Ku is due to its function in telomere protections rather than its role in NHEJ. Loss of Ku in human cells has previously been associated with dramatic telomere loss (82, 83). Future experiments will reveal if our conditional knockout will display phenotypes that are in concordance with previous findings.

RPE1 cells were immortalized through the introduction of telomerase into retinal pigmentation cells. Thus, they display genomic stability, growth characteristics, and gene expression patterns that mimic young normal cells (45). HEK293 cells show greater polyploidy and genome instability that suggests a greater reliance on DNA repair mechanisms, namely NHEJ which is the major DSB repair process in mammals (23, 44). This could be a confounding variable while trying to generalize conclusions about Ku gathered from HEK293 cells to all human cells. Although attempts to create an RPE1

conditional Ku70 knockout were not successful in this project, that goal should be further pursued as diploid RPE1 cells would be more representative of 'normal' human cells compared to polyploid HEK293 cells.

As many cellular functions of Ku are yet not well characterized, using an enzyme-catalyzed proximity system such as proximity-dependent biotin identification (BioID) has been used to reveal less known and yet to be discovered transient interactors of Ku (84). Mutant forms of Ku70 or BioID-tagged Ku70 can be stably integrated into these knockout cell lines to further study the function of Ku70 without interference from highly expressed, endogenous Ku70. Further studies should be conducted to compare the interactome of Ku in humans with mice and other organisms where Ku has been successfully knocked out to understand why Ku appears to be essential in humans. Advances in BioID have produced TurboID, which can label interactors in matters of minutes as compared to 18 hours required by BioID (85, 86). This could be paired with mass spectrometry to capture a snapshot of the Ku interactome under specific cellular conditions, such as during the repair of DSBs to better understand Ku in the context of DNA repair.

To improve gene editing efficiencies of either SaCas9 or TevSaCas9, the method of introducing TevSaCas9 and SaCas9 may be switched from plasmid transfection to using electroporation to directly deliver TevCas9 and Cas9 complexed with synthetic gRNA into cells. Using the protein version of Cas9 has been shown to increase cleavage compared to Cas9 delivered into cells on a plasmid (87). The process of selecting monoclonal cell lines can also be optimized by using fluorescence activated cell sorting (FACS) instead of antibiotic selection. FACS is comparatively faster (88) and less likely to produce false

positives as the nuclease and GFP are under the same promoter in our plasmid constructs but the antibiotic resistance marker is controlled by its own promoter.

4.9   Conclusion

The knockout strategy employed in this work can be generalized to knockout other highly expressed genes that may have multiple pseudogenes present in the genome. Pseudogenes do not contain exons; thus, introns can be targeted near an intron-exon junction. With TevCas9, it is possible to get cleavage in the exon itself, while only targeting the intron. With Cas9, this is much less likely and dependent on error-prone exonucleolytic processing to create deletions large enough to extend into the exon, demonstrating the versatility of using TevCas9 in addressing more challenging knockout targets.

Ku70 plays an important role in the NHEJ repair pathway. Ku70 knockout has already been achieved in mouse cells and used to link Ku-deficiency to increased cancer incidence and early onset of aging (17). However, studying Ku is difficult in human cells without a Ku70 knockout human cell line. We were able to create a conditional knockout of Ku70. This cell line can be used to investigate if Ku is essential in HEK293 cells. If found to be essential, this would be consistent with previous findings that indicated that knocking out Ku70 is lethal in other human cell lines and the lack of a single patient with a Ku70 or Ku80 genetic disease related mutation (17, 39, 42, 68). The conditional Ku70 knockout created in this project can serve as the basis for studies further investigating other cellular roles of Ku outside of NHEJ, such as telomerase maintenance, and why Ku only appears to be indispensable for human cell viability.

References

1. Lindahl, T., and Barnes, D. E. (2000) Repair of endogenous DNA damage. *Cold Spring Harb. Symp. Quant. Biol.* **65**, 127–133

2. Jackson, S. P., and Bartek, J. (2009) The DNA-damage response in human biology and disease. *Nature*. **461**, 1071–1078

3. Lieber, M. R. (2010) The Mechanism of Double-Strand DNA Break Repair by the Nonhomologous DNA End Joining Pathway. *Annu Rev Biochem*. **79**, 181–211

4. Kawanishi, S., Hiraku, Y., Pinlaor, S., and Ma, N. (2006) Oxidative and nitrative DNA damage in animals and patients with inflammatory diseases in relation to inflammation-related carcinogenesis. *Biol. Chem.* **387**, 365–372

5. Valko, M., Rhodes, C. J., Moncol, J., Izakovic, M., and Mazur, M. (2006) Free radicals, metals and antioxidants in oxidative stress-induced cancer. *Chem. Biol. Interact.* **160**, 1–40

6. O'Driscoll, M. (2012) Diseases Associated with Defective Responses to DNA Damage. *Cold Spring Harb Perspect Biol*. **4**, 1–26

7. Yi, C., and He, C. (2013) DNA Repair by Reversal of DNA Damage. *Cold Spring Harb Perspect Biol*. **5**, a012575

8. Jiricny, J. (2006) The multifaceted mismatch-repair system. *Nat. Rev. Mol. Cell Biol.* **7**, 335–346

9. David, S. S., O'Shea, V. L., and Kundu, S. (2007) Base-excision repair of oxidative DNA damage. *Nature*. **447**, 941–950

10. Hoeijmakers, J. H. (2001) Genome maintenance mechanisms for preventing cancer. *Nature*. **411**, 366–374

11. Goodman, M. F., and Woodgate, R. (2013) Translesion DNA Polymerases. *Cold Spring Harbor Perspectives in Biology*. **5**, a010363–a010363

12. Roth, D. B. (2014) V(D)J Recombination: Mechanism, Errors, and Fidelity. *Microbiology Spectrum*. **2**, 1–19

13. Watt, P. M., and Hickson, I. D. (1994) Structure and function of type II DNA topoisomerases. *Biochem J*. **303**, 681–695

14. Matos, J., and West, S. C. (2014) Holliday junction resolution: Regulation in space and time. *DNA Repair*. **19**, 176–181

15. Cortés-Ledesma, F., and Aguilera, A. (2006) Double-strand breaks arising by replication through a nick are repaired by cohesin-dependent sister-chromatid exchange. *EMBO Rep.* **7**, 919–926

16. San Filippo, J., Sung, P., and Klein, H. (2008) Mechanism of Eukaryotic Homologous Recombination. *Annu. Rev. Biochem.* **77**, 229–257

17. Fell, V. L., and Schild-Poulter, C. (2015) The Ku heterodimer: Function in DNA repair and beyond. *Mutation Research/Reviews in Mutation Research.* **763**, 15–29

18. Frit, P., Ropars, V., Modesti, M., Charbonnier, J.-B., and Calsou, P. (2019) Plugged into the Ku-DNA hub: The NHEJ network. *Progress in Biophysics and Molecular Biology.* **147**, 62–76

19. Gu, Y., Jin, S., Gao, Y., Weaver, D. T., and Alt, F. W. (1997) Ku70-deficient embryonic stem cells have increased ionizing radiosensivity, defective DNA end-binding activity, and inability to support V(D)J recombination. *Proc. Natl. Acad. Sci. U.S.A.* **94**, 8076–8081

20. Singleton, B. K., Priestley, A., Steingrimsdottir, H., Gell, D., Blunt, T., Jackson, S. P., Lehmann, A. R., and Jeggo, P. A. (1997) Molecular and biochemical characterization of xrs mutants defective in Ku80. *Mol. Cell. Biol.* **17**, 1264–1273

21. Weterings, E., and Chen, D. J. (2008) The endless tale of non-homologous end-joining. *Cell Res.* **18**, 114–124

22. Aravind, L., and Koonin, E. V. (2001) Prokaryotic Homologs of the Eukaryotic DNA-End-Binding Protein Ku, Novel Domains in the Ku Protein and Prediction of a Prokaryotic Double-Strand Break Repair System. *Genome Res.* **11**, 1365–1374

23. Mao, Z., Bozzella, M., Seluanov, A., and Gorbunova, V. (2008) DNA repair by nonhomologous end joining and homologous recombination during cell cycle in human cells. *Cell Cycle.* **7**, 2902–2906

24. Shibata, A., Jeggo, P., and Löbrich, M. (2018) The pendulum of the Ku-Ku clock. *DNA Repair.* **71**, 164–171

25. Wang, C., and Lees-Miller, S. P. (2013) Detection and repair of ionizing radiation-induced DNA double strand breaks: new developments in nonhomologous end joining. *Int. J. Radiat. Oncol. Biol. Phys.* **86**, 440–449

26. Povirk, L. F. (2012) Processing of damaged DNA ends for double-strand break repair in mammalian cells. *ISRN Mol Biol.* **2012**, 1–16

27. Postow, L., Ghenoiu, C., Woo, E. M., Krutchinsky, A. N., Chait, B. T., and Funabiki, H. (2008) Ku80 removal from DNA through double strand break–induced ubiquitylation. *The Journal of Cell Biology.* **182**, 467–479

28. Feng, L., and Chen, J. (2012) The E3 ligase RNF8 regulates KU80 removal and NHEJ repair. *Nature Structural & Molecular Biology*. **19**, 201–206

29. Wu, D., Topper, L. M., and Wilson, T. E. (2008) Recruitment and dissociation of nonhomologous end joining proteins at a DNA double-strand break in Saccharomyces cerevisiae. *Genetics*. **178**, 1237–1249

30. Williams, J. M., Ouenzar, F., Lemon, L. D., Chartrand, P., and Bertuch, A. A. (2014) The Principal Role of Ku in Telomere Length Maintenance Is Promotion of Est1 Association with Telomeres. *Genetics*. **197**, 1123–1136

31. Lemon, L. D., Morris, D. K., and Bertuch, A. A. (2019) Loss of Ku's DNA end binding activity affects telomere length via destabilizing telomere-bound Est1 rather than altering TLC1 homeostasis. *Sci Rep*. **9**, 1–13

32. Chen, H., Xue, J., Churikov, D., Hass, E. P., Shi, S., Lemon, L. D., Luciano, P., Bertuch, A. A., Zappulla, D. C., Géli, V., Wu, J., and Lei, M. (2018) Structural Insights into Yeast Telomerase Recruitment to Telomeres. *Cell*. **172**, 331–343

33. Teo, S. H., and Jackson, S. P. (1997) Identification of Saccharomyces cerevisiae DNA ligase IV: involvement in DNA double-strand break repair. *EMBO J.* **16**, 4788–4795

34. d'Adda di Fagagna, F., Hande, M. P., Tong, W. M., Roth, D., Lansdorp, P. M., Wang, Z. Q., and Jackson, S. P. (2001) Effects of DNA nonhomologous end-joining factors on telomere length and chromosomal stability in mammalian cells. *Curr. Biol.* **11**, 1192–1196

35. Vogel, H., Lim, D.-S., Karsenty, G., Finegold, M., and Hasty, P. (1999) Deletion of Ku86 causes early onset of senescence in mice. *PNAS*. **96**, 10770–10775

36. Vandersickel, V., Mancini, M., Slabbert, J., Marras, E., Thierens, H., Perletti, G., and Vral, A. (2010) The radiosensitizing effect of Ku70/80 knockdown in MCF10A cells irradiated with X-rays and p(66)+Be(40) neutrons. *Radiat Oncol*. **5**, 30

37. De Zio, D., Bordi, M., Tino, E., Lanzuolo, C., Ferraro, E., Mora, E., Ciccosanti, F., Fimia, G. M., Orlando, V., and Cecconi, F. (2011) The DNA repair complex Ku70/86 modulates Apaf1 expression upon DNA damage. *Cell Death Differ*. **18**, 516–527

38. Zheng, Y., Ao, Z., Wang, B., Jayappa, K. D., and Yao, X. (2011) Host Protein Ku70 Binds and Protects HIV-1 Integrase from Proteasomal Degradation and Is Required for HIV Replication. *J. Biol. Chem.* **286**, 17722–17735

39. Ghosh, G., Li, G., Myung, K., and Hendrickson, E. A. (2007) The lethality of Ku86 (XRCC5) loss-of-function mutations in human cells is independent of p53 (TP53). *Radiation research*. **167**, 66–79

40. Li, G., Nelsen, C., and Hendrickson, E. A. (2002) Ku86 is essential in human somatic cells. *Proceedings of the National Academy of Sciences*. **99**, 832–837

41. Fattah, K. R., Ruis, B. L., and Hendrickson, E. A. (2008) Mutations to Ku reveal differences in human somatic cell lines. *DNA Repair*. **7**, 762–774

42. Blomen, V. A., Májek, P., Jae, L. T., Bigenzahn, J. W., Nieuwenhuis, J., Staring, J., Sacco, R., Diemen, F. R. van, Olk, N., Stukalov, A., Marceau, C., Janssen, H., Carette, J. E., Bennett, K. L., Colinge, J., Superti-Furga, G., and Brummelkamp, T. R. (2015) Gene essentiality and synthetic lethality in haploid human cells. *Science*. **350**, 1092–1096

43. Thomas, P., and Smart, T. G. (2005) HEK293 cell line: A vehicle for the expression of recombinant proteins. *Journal of Pharmacological and Toxicological Methods*. **51**, 187–200

44. Lin, Y.-C., Boone, M., Meuris, L., Lemmens, I., Van Roy, N., Soete, A., Reumers, J., Moisse, M., Plaisance, S., Drmanac, R., Chen, J., Speleman, F., Lambrechts, D., Van de Peer, Y., Tavernier, J., and Callewaert, N. (2014) Genome dynamics of the human embryonic kidney 293 lineage in response to cell biology manipulations. *Nature Communications*. **5**, 1–12

45. Bodnar, A. G. (1998) Extension of Life-Span by Introduction of Telomerase into Normal Human Cells. *Science*. **279**, 349–352

46. Jinek, M., Chylinski, K., Fonfara, I., Hauer, M., Doudna, J. A., and Charpentier, E. (2012) A Programmable Dual-RNA—Guided DNA Endonuclease in Adaptive Bacterial Immunity. *Science*. **337**, 816–821

47. Paul, W. E. (2011) Bridging Innate and Adaptive Immunity. *Cell*. **147**, 1212–1215

48. Shah, S. A., Erdmann, S., Mojica, F. J. M., and Garrett, R. A. (2013) Protospacer recognition motifs. *RNA Biol*. **10**, 891–899

49. Mali, P., Yang, L., Esvelt, K. M., Aach, J., Guell, M., DiCarlo, J. E., Norville, J. E., and Church, G. M. (2013) RNA-Guided Human Genome Engineering via Cas9. *Science*. **339**, 823–826

50. Ran, F. A., Hsu, P. D., Wright, J., Agarwala, V., Scott, D. A., and Zhang, F. (2013) Genome engineering using the CRISPR-Cas9 system. *Nat. Protocols*. **8**, 2281–2308

51. Ran, F. A., Cong, L., Yan, W. X., Scott, D. A., Gootenberg, J. S., Kriz, A. J., Zetsche, B., Shalem, O., Wu, X., Makarova, K. S., Koonin, E. V., Sharp, P. A., and Zhang, F. (2015) *In vivo* genome editing using Staphylococcus aureus Cas9. *Nature*. **520**, 186–191

52. Kaya, H., Mikami, M., Endo, A., Endo, M., and Toki, S. (2016) Highly specific targeted mutagenesis in plants using *Staphylococcus aureus* Cas9. *Scientific Reports*. **6**, 26871

53. Wolfs, J. M., Hamilton, T. A., Lant, J. T., Laforet, M., Zhang, J., Salemi, L. M., Gloor, G. B., Schild-Poulter, C., and Edgell, D. R. (2016) Biasing genome-editing events toward precise length deletions with an RNA-guided TevCas9 dual nuclease. *Proceedings of the National Academy of Sciences*. **113**, 14988–14993

54. Roey, P. V., Belfort, M., and Derbyshire, V. (2013) *Homing Endonuclease I-TevI: An Atypical Zinc Finger with a Novel Function*, Landes Bioscience, Georgetown

55. Kleinstiver, B. P., Wolfs, J. M., Kolaczyk, T., Roberts, A. K., Hu, S. X., and Edgell, D. R. (2012) Monomeric site-specific nucleases for genome editing. *PNAS*. **109**, 8061–8066

56. Pink, R. C., Wicks, K., Caley, D. P., Punch, E. K., Jacobs, L., and Francisco Carter, D. R. (2011) Pseudogenes: Pseudo-functional or key regulators in health and disease? *RNA*. **17**, 792–798

57. Cooke, S. L., Shlien, A., Marshall, J., Pipinikas, C. P., Martincorena, I., Tubio, J. M. C., Li, Y., Menzies, A., Mudie, L., Ramakrishna, M., Bignell, G. R., Tarpey, P. S., Behjati, S., Nik-Zainal, S., Papaemmanuil, E., Teixeira, V. H., Raine, K., O'Meara, S., Dodoran, M. S., Butler, A. P., Iacobuzio-Donahue, C., Santarius, T., Grundy, R. G., Malkin, D., Greaves, M., Munshi, N., Flanagan, A. M., Bowtell, D., Martin, S., Larsimont, D., Reis-Filho, J. S., Boussioutas, A., Taylor, J. A., Hayes, N. D., Janes, S. M., Futreal, P. A., Stratton, M. R., McDermott, U., Campbell, P. J., and Group, I. B. C. (2014) Processed pseudogenes acquired somatically during cancer development. *Nature Communications*. **5**, 3644

58. Pink, R. C., and Carter, D. R. F. (2013) Pseudogenes as regulators of biological function. *Essays In Biochemistry*. **54**, 103–112

59. Richardson, C., and Jasin, M. (2000) Frequent chromosomal translocations induced by DNA double-strand breaks. *Nature*. **405**, 697–700

60. Strathdee, C. A., McLeod, M. R., and Hall, J. R. (1999) Efficient control of tetracycline-responsive gene expression from an autoregulated bi-directional expression vector. *Gene*. **229**, 21–29

61. Engler, C., Kandzia, R., and Marillonnet, S. (2008) A One Pot, One Step, Precision Cloning Method with High Throughput Capability. *PLOS ONE*. **3**, e3647

64. Brinkman, E. K., Chen, T., Amendola, M., and van Steensel, B. (2014) Easy quantitative assessment of genome editing by sequence trace decomposition. *Nucleic Acids Res*. **42**, e168–e168

65. Mahmood, T., and Yang, P.-C. (2012) Western Blot: Technique, Theory, and Trouble Shooting. *N Am J Med Sci*. **4**, 429–434

66. Bradford, M. M. (1976) A rapid and sensitive method for the quantitation of microgram quantities of protein utilizing the principle of protein-dye binding. *Anal. Biochem.* **72**, 248–254

67. Singleton, B. K., Priestley, A., Steingrimsdottir, H., Gell, D., Blunt, T., Jackson, S. P., Lehmann, A. R., and Jeggo, P. A. (1997) Molecular and biochemical characterization of xrs mutants defective in Ku80. *Mol. Cell. Biol.* **17**, 1264–1273

68. Fattah, F. J., Lichter, N. F., Fattah, K. R., Oh, S., and Hendrickson, E. A. (2008) Ku70, an essential gene, modulates the frequency of rAAV-mediated gene targeting in human somatic cells. *PNAS*. **105**, 8703–8708

69. Allen, F., Crepaldi, L., Alsinet, C., Strong, A. J., Kleshchevnikov, V., De Angeli, P., Páleníková, P., Khodak, A., Kiselev, V., Kosicki, M., Bassett, A. R., Harding, H., Galanty, Y., Muñoz-Martínez, F., Metzakopian, E., Jackson, S. P., and Parts, L. (2019) Predicting the mutations generated by repair of Cas9-induced double-strand breaks. *Nat Biotechnol*. **37**, 64–72

70. Gomez-Martinez, M., Schmitz, D., and Hergovich, A. (2013) Generation of stable human cell lines with Tetracycline-inducible (Tet-on) shRNA or cDNA expression. *J Vis Exp*. **73**, e50171

71. Myung, K., Ghosh, G., Fattah, F. J., Li, G., Kim, H., Dutia, A., Pak, E., Smith, S., and Hendrickson, E. A. (2004) Regulation of Telomere Length and Suppression of Genomic Instability in Human Somatic Cells by Ku86. *Molecular and Cellular Biology*. **24**, 5050–5059

72. Park, S.-J., Ciccone, S. L. M., Freie, B., Kurimasa, A., Chen, D. J., Li, G. C., Clapp, D. W., and Lee, S.-H. (2004) A Positive Role for the Ku Complex in DNA Replication Following Strand Break Damage in Mammals. *J. Biol. Chem.* **279**, 6046–6055

73. Smirnov, E., Kalmárová, M., Koberna, K., Zemanová, Z., Malínský, J., Masata, M., Cvacková, Z., Michalová, K., and Raska, I. (2006) NORs and their transcription competence during the cell cycle. *Folia Biol. (Praha)*. **52**, 59–70

74. Stepanenko, A. A., and Dmitrenko, V. V. (2015) HEK293 in cell biology and cancer research: phenotype, karyotype, tumorigenicity, and stress-induced genome-phenotype evolution. *Gene*. **569**, 182–190

75. Klein, A., Miera, O., Bauer, O., Golfier, S., and Schriever, F. (2000) Chemosensitivity of B cell chronic lymphocytic leukemia and correlated expression of proteins regulating apoptosis, cell cycle and DNA repair. *Leukemia*. **14**, 40–46

76. Pucci, S., Mazzarelli, P., Rabitti, C., Giai, M., Gallucci, M., Flammia, G., Alcini, A., Altomare, V., and Fazio, V. M. (2001) Tumor specific modulation of KU70/80 DNA binding activity in breast and bladder human tumor biopsies. *Oncogene*. **20**, 739–747

77. Lemos, B. R., Kaplan, A. C., Bae, J. E., Ferrazzoli, A. E., Kuo, J., Anand, R. P., Waterman, D. P., and Haber, J. E. (2018) CRISPR/Cas9 cleavages in budding yeast reveal templated insertions and strand-specific insertion/deletion profiles. *Proc. Natl. Acad. Sci. U.S.A.* **115**, E2040–E2047

78. Haapaniemi, E., Botla, S., Persson, J., Schmierer, B., and Taipale, J. (2018) CRISPR–Cas9 genome editing induces a p53-mediated DNA damage response. *Nat Med*. **24**, 927–930

79. Enzmann, V., Hollborn, M., Poschinger, K., Wiedemann, P., and Kohen, L. (2001) Immunosuppression by IL-10-transfected human retinal pigment epithelial cells in vitro. *Current Eye Research*. **23**, 98–105

80. Piganeau, M., Ghezraoui, H., De Cian, A., Guittat, L., Tomishima, M., Perrouault, L., Rene, O., Katibah, G. E., Zhang, L., Holmes, M. C., Doyon, Y., Concordet, J.-P., Giovannangeli, C., Jasin, M., and Brunet, E. (2013) Cancer translocations in human cells induced by zinc finger and TALE nucleases. *Genome Research*. **23**, 1182–1193

81. Kreiss, P. (1999) Plasmid DNA size does not affect the physicochemical properties of lipoplexes but modulates gene transfer efficiency. *Nucleic Acids Research*. **27**, 3792–3798

82. Indiviglio, S. M., and Bertuch, A. A. (2009) Ku's essential role in keeping telomeres intact. *Proceedings of the National Academy of Sciences*. **106**, 12217–12218

83. Wang, Y., Ghosh, G., and Hendrickson, E. A. (2009) Ku86 represses lethal telomere deletion events in human somatic cells. *Proceedings of the National Academy of Sciences*. **106**, 12430–12435

84. Abbasi, S., and Schild-Poulter, C. (2019) Mapping the Ku Interactome Using Proximity-Dependent Biotin Identification in Human Cells. *J. Proteome Res.* **18**, 1064–1077

85. Branon, T. C., Bosch, J. A., Sanchez, A. D., Udeshi, N. D., Svinkina, T., Carr, S. A., Feldman, J. L., Perrimon, N., and Ting, A. Y. (2018) Efficient proximity labeling in living cells and organisms with TurboID. *Nat Biotechnol*. **36**, 880–887

86. Trinkle-Mulcahy, L. (2019) Recent advances in proximity-based labeling methods for interactome mapping. *F1000Res*. **8**, 135

87. Liang, X., Potter, J., Kumar, S., Zou, Y., Quintanilla, R., Sridharan, M., Carte, J., Chen, W., Roark, N., Ranganathan, S., Ravinder, N., and Chesnut, J. D. (2015)

Rapid and highly efficient mammalian cell engineering via Cas9 protein transfection. *Journal of Biotechnology*. **208**, 44–53

88. Akhmaltdinova, L., Lavrinenko, A., and Belyayev, I. (2017) Flow Cytometry in Detecting Resistant E. Coli Strains. *OAMJMS*. **5**, 592–594

Curriculum Vitae

Name:	Gursimran Parmar
Post-secondary Education and Degrees:	Western University London, Ontario, Canada 2014-2018 B.MSc. Western University London, Ontario, Canada 2018-2020 M.Sc.
Honours and Awards	Western Scholarship of Excellence 2014 Dean's Honour List 2014-2018 Western Scholars 2014-2018 Ontario Graduate Scholarship: Queen Elizabeth II (OGS-QEII) 2018 Travel award: Canadian Symposium on Telomeres and Genome Integrity 2019

Abstracts

Parmar, G, Edgell, D, Schild-Poulter C. Knockout of Ku70 in human cells using CRISPR/Cas9 and TevCas9.
Canadian Symposium on Telomeres and Genome Integrity
Montreal, ON
2018

Parmar, G, Edgell, D, Schild-Poulter C. Knockout of Ku70 in human cells using CRISPR/Cas9 and TevCas9.
London Health Research Day
London, ON
2018

Parmar, G, Edgell, D, Schild-Poulter C. Knockout of Ku70 in human cells using
CRISPR/Cas9 and TevCas9.
London Health Research Day
London, ON
2019

Parmar, G, Edgell, D, Schild-Poulter C. Knockout of Ku70 in human cells using
CRISPR/Cas9 and TevCas9.
Toronto DNA Replication and Repair Symposium
Toronto, ON
2019